Distribution Agreement

In presenting this thesis or dissertation as a partial fulfillment of the requirements for an advanced degree from Emory University, I hereby grant to Emory University and its agents the non-exclusive license to archive, make accessible, and display my thesis or dissertation in whole or in part in all forms of media, now or hereafter known, including display on the world wide web. I understand that I may select some access restrictions as part of the online submission of this thesis or dissertation. I retain all ownership rights to the copyright of the thesis or dissertation. I also retain the right to use in future works (such as articles or books) all or part of this thesis or dissertation.

Signature:

_____ Date:

June Woo

Studying the combination of CAR T cells and ICI for treatment of Melanoma

By

June Woo

Master of Science

Graduate Division of Biological and Biomedical Sciences

Cancer Biology

_____
Sarwish Rafiq Ph.D
Advisor

_____
Chrystal M. Paulos Ph.D
Committee Member

_____
H. Trent Spencer Ph.D
Committee Member

_____
Haydn T. Kissick Ph.D
Committee Member

_____
Kimberly Jacob Arriola Ph.D
Dean of the James T. Laney School of Graduate Studies

_____
Date

Studying the Combination of CAR T cells and ICI for treatment of Melanoma

By

June Woo
B.S., Emory University, 2022

Advisor:
Sarwish Rafiq, Ph.D

An abstract of
A thesis submitted to the Faculty of the James T. Laney School of Graduate Studies of Emory University in partial fulfillment of the requirements for the degree of Master of Science in the Graduate Division of Biology and Biomedical Sciences, Cancer Biology, 2023.

Abstract

Melanoma proves to be the most aggressive form of skin cancer due to its metastatic ability. Both CAR T cell therapy and immune checkpoint inhibitor (ICI) have seen great progress with the treatment for melanoma, but both therapies have toxicities related to treatment. Due to the limitations of both CAR T cell and ICI therapy, we aim to increase the efficacy of CAR T cell therapy by combining both treatments. Because Muc16CD is a suitable TAA and the anti-Muc16CDCAR has been validated in combination with anti-PD-1 in an ovarian cancer, we decided to use the same combination treatments in a melanoma model. Thus, we hypothesize that the combination of CAR T and ICI treatments would address the limitations of CAR and ICI therapies: CAR T cells would be able to direct an immune response against cold tumors while ICI could mount a response against the suppressive TME. Furthermore, we demonstrated this treatment in a clinically relevant model of melanoma called the YUMM cell line with a Braf/Pten mutations. We investigated CAR T cell function by testing its cytotoxic function, cytokine levels, proliferating and activating capabilities against YUMM tumors. We also tested the *in vitro* and *in vivo* characteristics of the YUMM cells that were taken from a GEMM model with a Braf activation and Pten inactivation mutations, mimicking melanoma seen in clinic. In *in vitro* assays, antigen-stimulated CAR T cells displayed an increase in cytokine levels, such as IFN-γ, and degranulation factors, such as CD107a and granzyme B compared to unstimulated CAR T cells. The anti-Muc16CD CAR was also able to specifically kill Muc16CD+ tumors *in vitro* compared to Muc16CD- tumor. And mouse CAR T cells were also more activated and proliferated when cultured with antigen-expressing cells. Because immunotherapy is a constantly growing field, combination of CAR T cell and ICI should be further studied in melanoma and solid tumors.

Table of Contents

Table of Figures

Introduction

Introduction

Melanoma

According to the CDC, melanoma is the third most common skin cancer. While it is less common than basal and squamous cancers, melanoma causes concern since it is the most likely skin cancer to metastasize to other parts of the body if not caught and treated early.[1] As of 2023, 186,680 cases of melanoma will be diagnosed and of those cases, 97,610 will be invasive while 89,070 cases will be noninvasive.[2]

Melanoma can occur when there is an overgrowth of melanocytes, which absorb UV light and sit at the basal level of the epidermis. 40% of hereditary melanoma occurs from CDKN2A mutations, which lead to defects in the cell cycle checkpoints.[3] Somatic mutations that can increase the risk of melanoma occur in the nucleotide excision repair pathways, which can be caused by UV radiation.[3] Risk factors such as having lighter skin, lighter hair color, and lighter eye colors have also been connected to developing melanoma.[3] Other mutations that are associated with melanoma occur in the MAPK signaling pathway, a key regulator of cell growth and proliferation.[4] Braf encodes for serine/threonine kinases that, when mutated, constitutively activates the MAPK pathway that leads to oncogenic cell growth.[4] Because MAPK kinase, also known as MEK, is phosphorylated by Braf, mutations in MEK also lead to oncogenic cell proliferation and survival.[4] Braf and MEK mutations are more likely to be found in patients younger than 30 years old than in patients older than 80 years old and patients with Braf mutated melanoma left untreated, generally has worse prognosis than Braf wild-type metastatic melanoma.[4]

For Braf-mutated melanoma patients, targeted therapy poses a good option for treatment.[5] However, certain Braf-targeted therapy responses are temporary, and patients can develop a resistance to Braf which subsequently can increase oncogenic cell growth.[4] As a result, MEK

inhibitors have also been developed and added in combination with Braf-targeted therapy since MEK follows Braf in the MAPK signaling pathway. Combination of Braf and MEK inhibitors have been safely tested in clinical I and II trials to overcome Braf resistance and proves to reduce incidence and severity in metastatic melanoma patients.[5] However, Braf mutations occur only in about 50% of melanoma patients which means that only select patients are eligible to receive targeted therapy treatments.[6] Consequently, the exploration, expansion, and improvement of other modes of treatment such as immune checkpoint inhibitors (ICI) and adoptive cell therapy are needed.

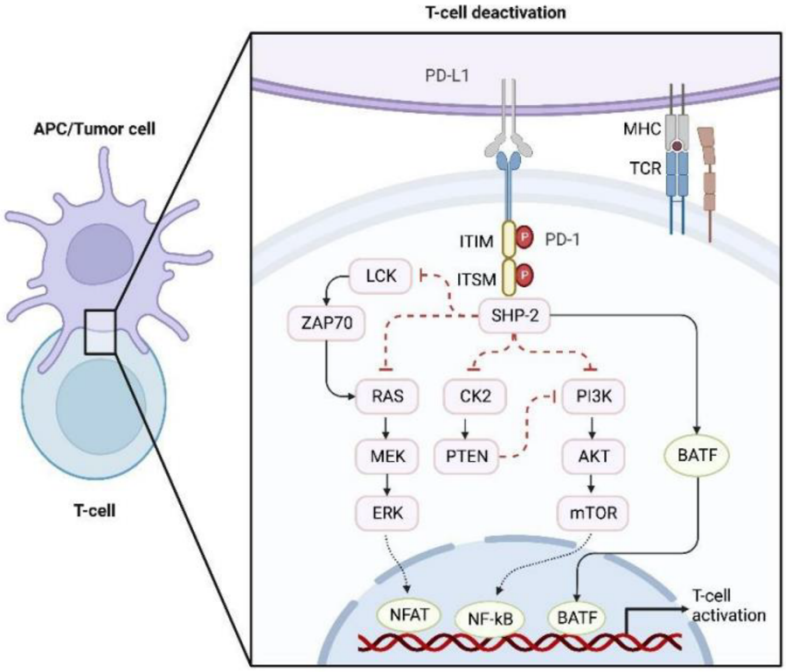

Fig. 1 | PD-1 and PD-L1 checkpoint proteins. PD-L1 from the APC or tumor cell binds to PD-1, activating the PD-1/PD-L1 pathway.[11] The PD-1/PD-L1 pathway prevents PI3K activation and also inhibits Ras, which is involved in the MAPK pathway. In this way T cell activation is inhibited and leads to T cell exhaustion. [11]

ICI Therapy

Immune checkpoints are a necessary part of the immune system to prevent immune responses from destroying healthy cells in the body. The checkpoints engage when proteins on T cells recognize and bind to partner proteins on other immune cells to provide an "off" signal.[7]

However, tumor cells evade immunosurveillance by activating the immune checkpoint pathways to suppress an antitumor response.[8] To combat this defense mechanism from tumors, antagonistic antibodies that serve as immune checkpoint inhibitors (ICI) have been developed as a type of immunotherapy that blocks regulatory proteins and results in preventing the immune system from "braking".

Programmed cell death protein-1 (PD-1) is an inhibitory receptor that is a checkpoint protein that binds to the immunoregulatory ligand, programmed cell death ligand 1 (PD-L1). Both PD-1 and PD-L1 are transmembrane proteins: PD-1 being expressed in immune cells such as T cells, B cells, macrophages, natural killer (NK) cells, dendritic cells, and monocytes.[9] and PD-L1 being expressed in lymphoid and non-lymphoid tissues as well as antigen-presenting cells (APC) and many tumor cells.[10] PD-1 is normally expressed on exhausted T cells and signals for the immune system to slow down. However, PD-1 expression also increases when T cell receptors recognize peptides on the MHC receptors on APC's, such as cancer cells.[9] PD-1 then inhibits T cell activation by preventing PI3K-Akt pathway and inhibiting MAPK pathway.[10] This refers to the tumors "adaptive immune mechanism," [9] that facilitates the PD-1/PD-L1 pathway and can express PD-L1 when alerted by the presence of T cells through the secretion of IFN-γ. Once PD-L1 is expressed, it binds to PD-1 on surrounding T cells and thus, enacts the "off" signal for the immune system (**Fig. 1**). Therefore, the PD-1/PD-L1 pathway controls and maintains the tumor's immune tolerance within the tumor microenvironment.[9]

Because the PD-1/PD-L1 pathway serve as a method of immune escape for tumors, anti-PD-1/PD-L1 monotherapy treatments have been developed to combat this defense. Anti-PD-1 monoclonal antibodies (mAb) work by binding to the PD-1 receptor on T cells due to its high affinity to PD-1 and blocking the PD-1 from interacting with the PD-L1.[12] This results in

constitutively active T cells. Anti-PD-L1 mAb's work by binding the PD-L1 receptor on APC's and blocking the PD-L1 from binding to the PD-1, which also causes the T cells to be constitutively active. Therefore, the anti-PD-1/PD-L1 mAb's create a defense method against tumor cells attempting to avoid immune surveillance.

The first monoclonal antibody FDA-approved for melanoma was ipilumumab targeting cytotoxic T-lymphocyte antigen-4 (CTLA-4) due to its durability and modest response in patients.[73] Subsequently, nivolumab and pembrolizumab were also FDA-approved due to general success in clinical trials. For example, in a phase I trial for patients with metastatic melanoma, nivolumab, an anti-PD-1 monotherapy drug, was tested in a patient cohort of n=39 where the drug was well tolerated and showed antitumor activity.[13] Since then, anti-PD-1 treatments, nivolumab and pembrolizumab, have been FDA-approved and over ipilimumab has become the first line treatment for metastatic melanoma since both nivolumab and pembrolizumab showed higher response rates and less toxicities compared to ipilimumab.[14,74] Other clinical trials involving anti-PD-L1 inhibitors also led to the FDA-approval of atezolizumab for the treatment of metastatic non-small cell lung cancer (NSCLC).[15]

Despite its promising clinical efficacy, ICI monotherapy has some limitations for melanoma. For example, certain cancer types can struggle to respond to ICI therapy in "cold" tumors or non-T cell inflamed cancers whereas a "hot" tumor can respond well to ICI therapy due to being T cell inflamed.[16] However, determining whether a tumor is "hot" or "cold" is not the only way to predict the clinical response to immunotherapy. To understand the clinical response to ICI therapy, we can classify tumors based on tumor mutational burden (TMB): high TMB is usually associated with a greater presence of neoantigens while a low TMB would have a lower presence of antigens that can be detected by the immune system.[16] Even though a high TMB relates

to having a higher number of neoantigens that can be detected by the immune system, a high TMB does not always indicate greater response rates to ICI therapy. Metastatic melanoma specifically has a high TMB but is less responsive to ICI making metastatic melanoma an immunologically "cold" tumor.[16] Thus, while TMB can be used to predict clinical response to ICI, there are other factors that are contributing to limited response rates of ICI therapy. One such factor is acquired resistance for ICI therapy use in melanoma as some patients will respond well to immune checkpoint in the beginning of treatment but become resistant over time during the treatment regimen.[17]

Fig. 2 | Current Strategies for CAR Design.[18]

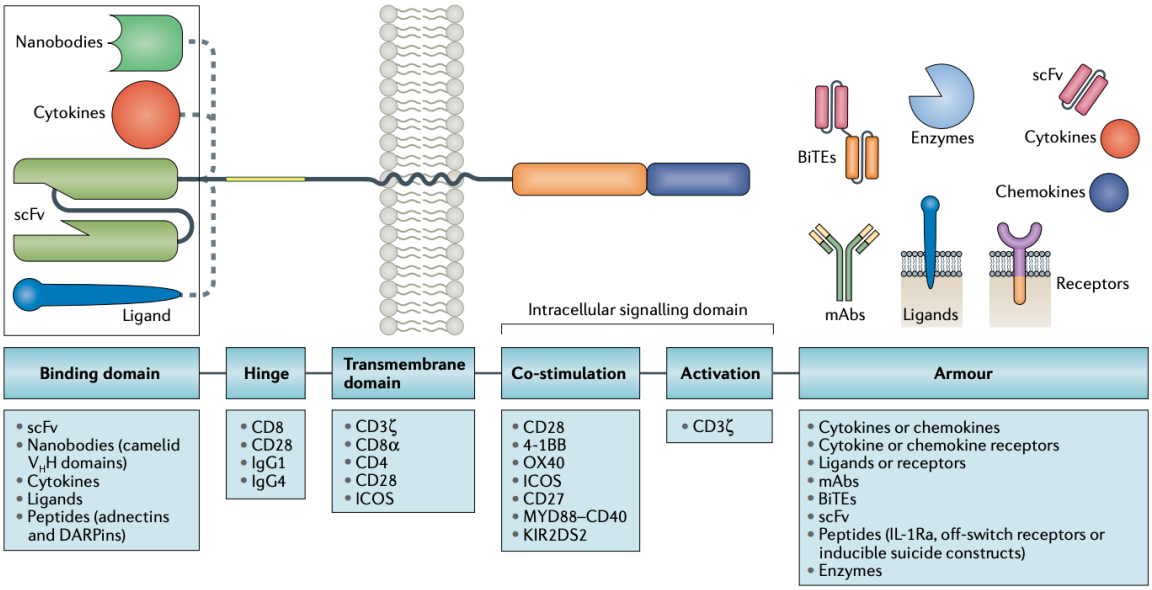

Another limitation of ICI therapy works exclusively with endogenous T cells meaning any patients with autoimmune disorders or any immunocompromised diseases would struggle to tolerate immunotherapy. Therefore, efforts to improve ICI therapy efficacy are required.

Adoptive Cell therapy (ACT)

Adoptive cell therapy (ACT) has been another heavily considered mode of treatment for solid tumors especially tumor infiltrating lymphocyte (TIL) therapy for melanoma. TIL therapy

involves removing tumor resident T cells from a patient, expanding the cells ex vivo, and then transferring it back into the same patient after undergoing a lymphodepleting regimen.[20] In 1988, the first demonstration of tumor-infiltrating lymphocyte (TIL) therapy showed promising clinical effects in patients with metastatic melanoma with the overall response rate being 60% in patients.[21] In clinical trials following the first TIL therapy treatment, response rates from patients reached up to 72% where 10-20% of treated patients reached complete remission.[22] An advantage to TIL therapy that leads to the efficient response rates in patients is its ability for the T cells to recognize defined and undefined tumor antigens allowing for broad major histocompatibility complex (MHC) coverage.[23] However, TIL therapy is associated with many toxicities during the preconditioning regimen, especially effects from lymphodepletion, involving a short round of chemotherapy to kill T cells.[20] Furthermore, like Braf-targeted therapy, a patient is only a good candidate for TIL therapy if enough TILs can be found at the tumor site and expanded.[24] Additionally, tumors can evade immune responses by downregulating MHC-1 complexes rendering naïve T cells unable to become effector cells.[25] This means that TIL therapy efficacy could decrease if there are defects in T cell priming caused by the tumor. Therefore, while TIL therapy offers broad antigen recognition, optimizing immunotherapy against melanoma is still a challenge and has brought light to other modes of immunotherapies such as chimeric antigen receptor (CAR) T cell therapy.

Chimeric Antigen Receptor T cells

Chimeric antigen receptor (CAR) T cell therapy is a type of ACT that involves engineering T cells to express a synthetic receptor with an extracellular antigen-binding domain that targets the desired tumor associated antigen (TAA). Engineering CARs call for piecing together different sequences involved in immune signaling and combining these parts to create the optimal antigen receptor. The extracellular domain typically consists of a single-chain variable fragment (scFv)

where a G4S linker connects variable light and variable heavy chains, derived from a monoclonal antibody (mAb) (**Fig.2**). In the CAR sequence itself, an mCD8a signal peptide is present to indicate the start codon for the scFv. Following the antigen-binding domain is the hinge and transmembrane domain to anchor the receptor to the membrane of the cell, which are typically sequences from CD8 and CD28 (**Fig. 2**). Inside the cell, the CAR consists of signaling domains where CD28 or 41BB are commonly used as a costimulatory signal and CD3ζ as an activation signal, mimicking TCR signaling (**Fig. 2**).

CAR T cell therapy has proven to be successful in hematological malignancies especially with the anti-CD19 CAR in B cell malignancies[26] and the anti-BCMA CAR T cells in multiple myeloma.[27] The CD19 antigen is a target of interest for B cell malignancies since it is expressed on the surface of B lymphocytes and more than 95% of B cell lymphomas express CD19.[28] Tisagenlecleucel, an anti-CD19 CAR T cell product, was first approved in 2017 for patients up to 25 years old with data supported by phase II ELIANA trial and University of Pennsylvania clinical trial, where 89% of their ALL patients had a complete response.[29,30] The FDA moved towards approval of anti-CD19 CAR T cell products for adult patients due to other clinical trial successes: in diffuse large B cell lymphoma (DLBCL), tisagenlecleucel had an overall response rate of 52%[31] and axicabtagene ciloleucel had a complete response rate of 58%.[32] In multiple myeloma, the B-cell maturation antigen (BCMA) is a favorable target since it is expressed on all malignant myeloma cells but not on normal tissue.[33] In the first clinical trial using the anti-BCMA CAR in humans, patients had an overall response rate of 81% and 63% were partial or complete.[27] Additionally, the KarMMa study, phase II trial, observed an overall response rate of 73% and a complete response rate of 33% for anti-BCMA CAR T cell treatment in multiple myeloma,[34] which

led to the basis of the FDA approval for idecabtagene vicleucel.[35] Thus, CAR T cell therapy has seen general clinical trial successes and FDA approvals for hematological malignancies.

However, the CAR T cell response rate for solid tumors have seen limited efficacy clinically compared to blood-related malignancies. For example, one clinical study that consisted of 24 melanoma patients was terminated early because there was no objective response to the treatment and the majority of patients showed progressive disease.[36] This is due to obstacles that solid tumors present to CAR T cells.

The tumor microenvironment (TME) for solid tumors is immunosuppressive since solid tumors can be infiltrated by different cells that promote tumor proliferation.[37] Melanoma have tumor-associated fibroblasts in their TME that assist with tumorigenesis by participating in the secretion of growth factors.[38] Regulatory T cells (Tregs) also act as barriers in the aggressive TME by producing TGF-B and IL-10 which are immunosuppressive cytokines and can hamper the cytolytic capacity of the TME.[39] Physical barriers in the TME also hampers the CAR T cell's ability to migrate and penetrate the solid tumor.[40] Furthermore, in the presence of IFN-γ, melanoma expresses the inhibitory ligand, PD-L1, to escape immune surveillance.[41] Moreover, another challenge for CAR T cell therapy against solid tumors is finding a suitable TAA. A unique TAA is very crucial to avoid on-target, off-tumor toxicities.[42] On-target, off-tumor (OTOT) toxicities occur when non-cancerous cells expressing the target antigen are killed by CAR T cells. Many clinical trials were terminated due to OTOT toxicities occurring in patients with solid tumors: patients with CEACAM5+ malignancies were treated with CEACAM5 specific CAR T cells and resulted in patients with a variety of adverse events.[43] Therefore, a good TAA candidate must not be expressed on non-malignant cells and should be exclusive to the tumor cells.[42] However, even after finding a specific antigen for the tumor, solid tumors can express the antigen at different

levels across tumor sites, referred to as tumor antigen heterogeneity.[37] Varying levels of antigen expression on solid tumors may decrease CAR T cell efficacy and makes it difficult to find the optimal target in the solid tumors.[37] Finally, another challenge for CAR T cell therapy against solid tumors is infiltrating the solid tumors. CAR T cells can encounter blood tumor cells more frequently since CAR T cells cycle through the lymphatic system and bloodstream, making solid tumors a harder reach for CAR T cells.[37] In addition, for metastatic melanoma, tumor cells activate oncogenic pathways such as β-catenin which prevents T cells from infiltrating the tumor site.[44] Thus, there are many roadblocks dampening CAR T cell therapies efficacy against solid tumors that need to be optimized and further studied.

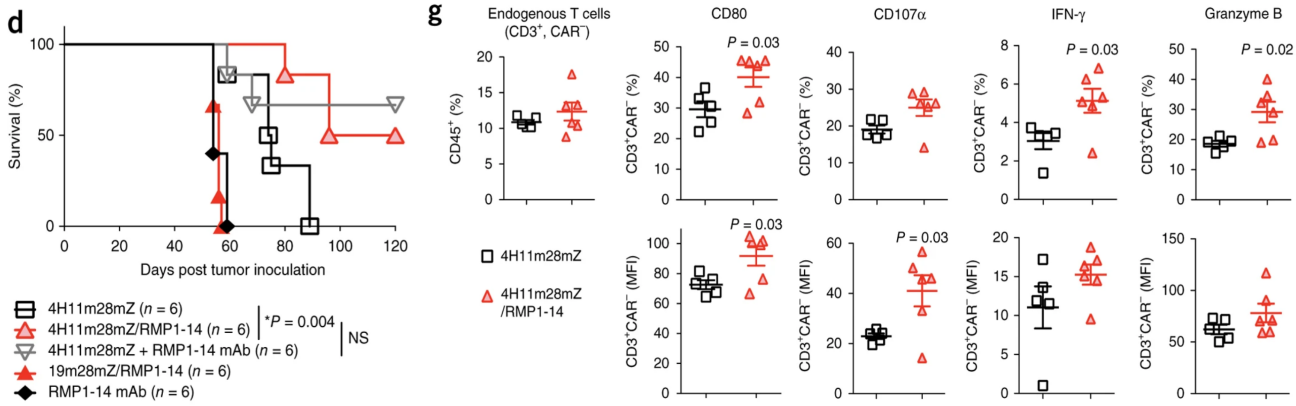

Fig. 3 | Anti-Muc16CD CAR has been validated in Muc16CD+ tumors.[3]

Muc16CD as a suitable target for CAR T cell therapy:

Notable CAR T cell targets for melanoma that have been developed for preclinical studies are as follows: CD126, CD70, B7-H3, HER2, VEGFR-2, gp100/HLA-A2, CSPG4, GD2, and GD3.[36] Muc16CD is also a potential TAA that has proven to be a suitable target for melanoma. Muc16 is a tree-like glycoprotein that consists of two parts: the ectodomain and the branch. When cleaved, the branch portion, classified as CA-125, enters the bloodstream and can be used as a biomarker of disease burden, relapse, or response to treatment (**Fig. 4**).[45] The ectodomain, Muc16CD, remains on the surface of cells and when upregulated, becomes oncogenic, often

expressed on ovarian carcinomas.[46] An anti-Muc16CD (4H11) second generation CAR (**Fig. 5**) has thus been developed to target Muc16CD in ovarian cancer and 4H11-28z CAR T cells have been able to display specific cytotoxic ability towards ovarian cancer cells in vitro.[46] A phase I clinical trial was also conducted to safely test and optimize the 4H11-28z CAR T cell efficacy.[47,48] Although an elimination gene was present, OTOT toxicities were not observed and the best response from the trial was stable disease[48] resulting in promising efficacy from the 4H11 CAR but also calling for the need to test new strategies with this CAR.

Since Muc16CD proves to be a suitable target for ovarian cancer, we wanted to see if this target would equally be suitable and relevant to melanoma to increase the CAR T cell treatment efficacy. Further analysis of Muc16 reveals that the Muc16 gene is one of the most mutated genes for melanoma and is correlated with TMB and immunotherapeutic efficacy.[49] Thus,

Fig. 4 | Schematic of Muc16 and the cleaved portions: CA-125 and the ectodomain of Muc16.

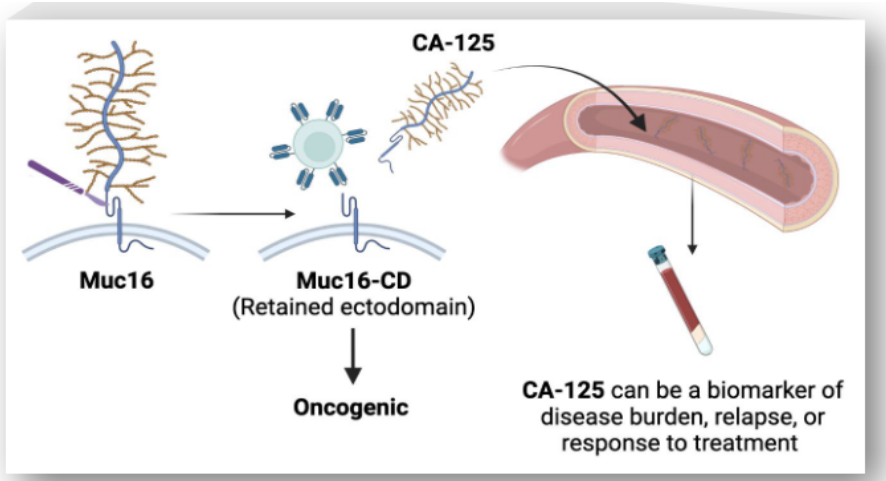

(Created in Biorender) *Biorender by Heather Lin*

(Rao et al 2010, Rao et al 2015, Das et al 2015)

Muc16 is a target worth investigating further especially because the anti-Muc16CD CAR has already been developed and validated for this TAA. For our studies, we are using this CAR as a

tool to evaluate the antitumor efficacy of combination of CAR T cell and ICI therapies in a melanoma model.

ACT and ICI

Many different combination strategies of ICI and ACT therapies have been studied in the treatment of solid tumors. In a clinical trial, anti-CTLA-4 antibody (ipilumumab) was used to treat ovarian cancer patients before tumors were harvested for TIL production.[50] The logic was that tumor infiltration would occur with ICI treatment before collecting TILs from the tumor site, thus allowing for better TIL production.[50] This approach resulted in more successful expansion of TILs (increased numbers of TILs), better CD8:CD4 ratio, and increased antitumor reactivity, thus proving that the combination of TIL therapy and ICI therapy was safe and improving the antitumor effect of TILs in patients.[50] A phase II trial also observed the effects of TIL therapy in combination with anti-PD-1 treatment (pembrolizumab) and found favorable response rates in a variety of solid tumors: 56.3% in melanoma, 87.5% in head and neck squamous cell carcinoma, and 42.9% in cervical cancer.[51]

Preclinical research involving CAR T cell and ICI combination therapy observed increased antitumor efficacy in vitro and in xenogeneic mouse models in an ovarian cancer model.[19] This study was also able to demonstrate the safe administration of CAR T cell mediated ICI therapy where anti-PD-1 scFv was secreted by CAR T cells allowing for localized anti-PD-1 treatment.[19] Furthermore, the study was able to validate the use of an anti-Muc16CD CAR in a solid tumor model (**Fig. 3**).

Fig. 5 | Anti-Muc16CD CAR Construct generated with an SFG-vector. This CAR construct is a second-generation CAR and was used for this study. The scFv includes the anti-Muc16CD portion and is the extracellular part of the CAR. Connected by a hinge protein, following the scFv is the CD28 transmembrane protein that anchors the CAR to the cell surface. The intracellular portion includes the CD28 and CD3ζ signaling domains responsible for T cell activation and killing ability.[18]

CAR T cell and ICI combination therapy has been tested clinically with promising results. In a phase I trial, patients with malignant pleural disease (MPM) received mesothelin-targeted CAR T cells in combination with anti-PD-1 treatment (atezolizumab) after observing that anti-PD-1 treatment enhanced CAR T cell function.[52] As a result, median overall survival was at 23.9 months and 8 out of 18 patients were able to sustain stable disease for over six months.[52] This study also demonstrated the safe administration of ICI and CAR T cell therapy and urged for more studies on combination of CAR T cell and ICI treatments on solid tumors. Ongoing clinical trials include one in the Shanghai Mengchao Cancer Hospital where an aPD-1 mesothelin CAR is being tested for safety and tolerability in mesothelin positive solid tumors as of May 2022 (unspecified).[54] Another ongoing clinical trial involves CAR T cells targeting claudin18.2 (CLDN18.2) with prior doses of anti-PD-1 treatment in digestive system cancers.[53] Interim results

reveal that patients who had received anti-PD-1 antibody prior to CAR T cell treatment had seen shrinkage of tumor lesion.[53]

Fig. 6 | Combination of ICI and CAR T Cell Therapies as a Strategy to Overcome Roadblocks.

Therefore, ACT in combination with ICI therapy has proven to be an effective way to increase ACT's antitumor efficacy with the idea that ICI therapy could help tumor infiltration on top of ACT administration, especially in a solid tumor model. Additionally, it adds the safety factor of administering these treatments.

Mouse Melanoma Models

To study melanoma, researchers use syngeneic mouse models since most of the mouse genes share the same functions as human genes therefore, making it easier to study gene

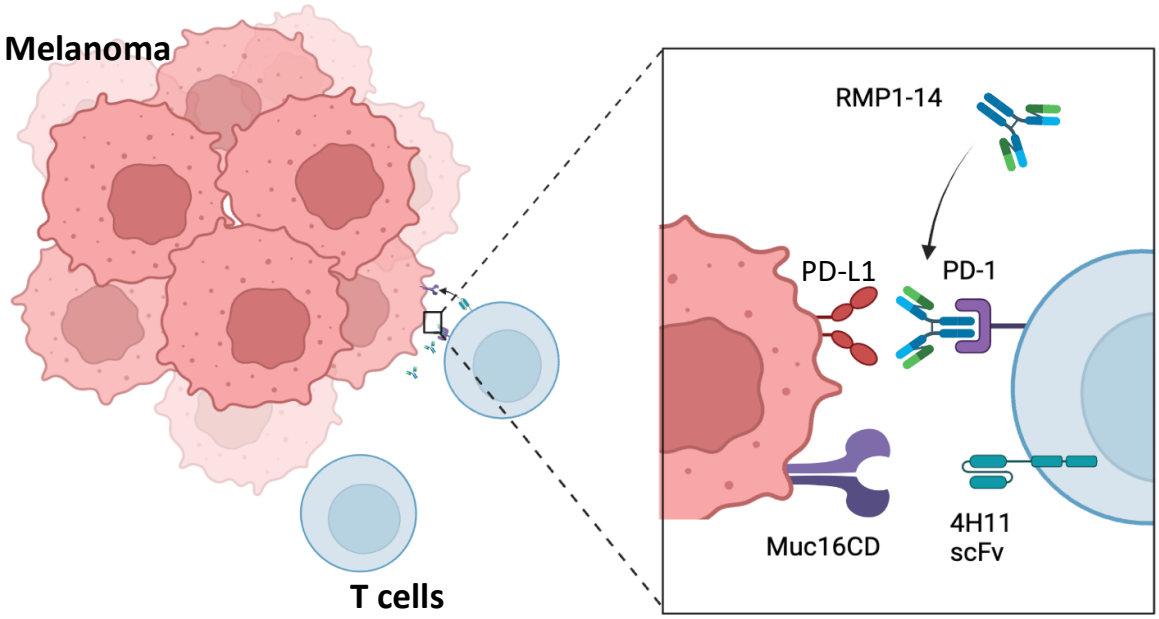

Made with Biorender

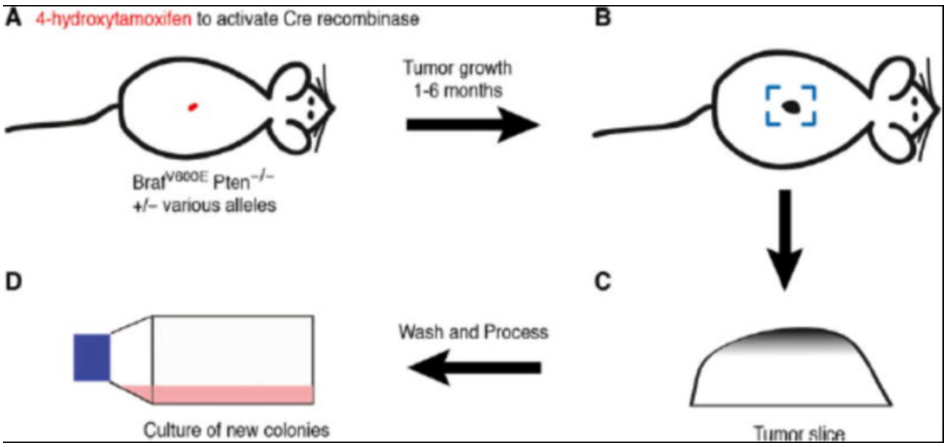

Fig. 7 | How the YUMM cells were cultured.[55]

mutations in a cost-effective preclinical model. B16 is a melanoma cell line that emerged spontaneously in the melanin-producing epithelia of a C7B5L/6J mouse in 1954.[56] Because of the B16's ability to metastasize to the lung, liver, and spleen, the B16 model is also used as a metastatic melanoma model.[56] Since then, the B16 model has been widely used to test treatments in preclinical studies. ICI treatments have also been studied in the B16 model and shown to be effective, especially in combined ICI therapies.[57] While B16 continues to be used for research, the model lacks clinical relevance due to its unique analogs, ambiguous genetic drivers, and having retroviral elements that could confound generalizability.[55] Therefore, the Yale University Mouse Melanoma (YUMM) lines have been developed with genetic drivers specific to human melanoma to be used in research as a clinically relevant murine melanoma model.[55] The YUMM cell lines were developed in a GEMM model that involved a Braf activation, Pten inactivation, and Cdk2NA inactivation.[55] After the tumors grew to $100mm^3$, the tumors were excised and cultured in DMEM (**Fig.7**).[55] Thus, allowing us to use the YUMM cell line for in a lab setting for its clinical relevance.

Due to the limitations of both CAR T cell and ICI therapy, we aim to increase the efficacy of CAR T cell therapy by combining both treatments (**Fig.6**). Because Muc16CD is a suitable TAA and the anti-Muc16CDCAR has been validated in combination with anti-PD-1 in an ovarian cancer, we decided to use the same combination treatments in a melanoma model. Thus, we hypothesize

that the combination of CAR T and ICI treatments would address the limitations of CAR and ICI therapies: CAR T cells would be able to direct an immune response against cold tumors while ICI could mount a response against the suppressive TME. Furthermore, we demonstrated this treatment in a clinically relevant model of melanoma called the YUMM cell line with a Braf/Pten mutations.

Materials and Methods

Materials and Methods:

Generation of viral vectors:

The anti-Muc16CD scFv sequence was designed by the Brentjens Lab. The gene was cloned in to the SFG retroviral vector containing the CD28 transmembrane and signaling domains CD28 and CD3ζ courtesy of the Brentjens Lab. The SFG-retroviral vector was used to encode the MUC16CD targeted CAR, termed SFG_4H11m28mZ.

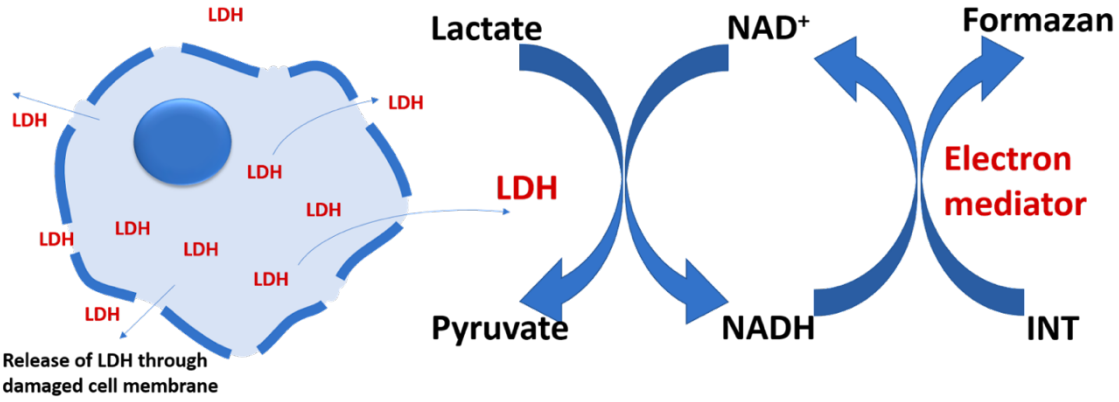

Fig. 8 | How LDH Assays Work. The LDH assay is based on an enzymatic coupling reaction. LDH catalyzes the conversion of lactate to pyruvate via NAD+ reduction to NADH. Diaphorase then uses NADH to reduce tetrazolium salt to a red formazan product that can be measured at 490 nm.[58]

Cell Culture:

Phoenix Eco packaging cells were obtained from the Brentjens Lab at Memorial Sloan Kettering. The Phoenix Eco packaging cells were cultured in DMEM supplemented. Tumor cells and mouse T cells were cultured in RPMI medium. All media was supplemented with 10% FBS, 2mM L-glutamine, 100 IU/mL penicillin and 100 ug/mL streptomycin. The retroviral construct encoding the anti-Muc16CD CAR were transiently transfected with H29 cells using calcium chloride. Once transfected, the H29 supernatant was filtered through a 0.45µg to remove the cells and then transduced with Phoenix Eco packaging cells to stably produce the retroviral producer cell lines (**Fig. 10**). The YUMM tumor cell line was acquired courtesy of the Paulos Lab.

Muc16CD was then overexpressed by transducing Phoenix Eco packaging cells containing the Muc16CD construct with the YUMM cell line. To ensure that Muc16CD was consistently being overexpressed in the YUMM cells, the YUMM-Muc16CD cell line was sorted by FACS based on high expression of Muc16CD following staining with PE-conjugated antibody for Muc16CD. All cells were routinely checked for mycoplasma.

Flow cytometry:

APC or FITC-conjugated primary antibodies, developed at the Memorial Sloan Kettering Cancer Center Antibody and Bioresource Core Facility, were used to detect the αMuc16CD scFv domain of the CAR construct. Data was collected using a Cytek Aurora spectral flow cytometer and transduction efficiency of transduced cells was analyzed with FlowJo v10.8 software.

Mouse splenocyte isolation and transduction:

Female C57BL/6 mice were ordered from Charles River Lab and used for mouse splenocyte isolation. On Day 1, the mouse was sacked with CO_2 and then the spleen was surgically removed and washed with PBS and resuspended in RPMI media (3% ATOS, 10% FBS). The T cells were then isolated from the spleens using RBC lysis and then activated using 1.0U/mL of IL-2 and 4μg/uL of concanavalin A. The mouse T cells were transduced with viral supernatant Phoenix Eco packaging cells for two consecutive days. On Day 4, mouse T cells were supplemented with RPMI media (3% ATOS, 10% FBS) and IL-2. Mouse T cell transduction efficiency was evaluated on flow cytometry. CAR T cells with a transduction efficiency of 20% or higher would be used for further study with *in vitro* functional assays or *in vivo* assays (**Fig.11**).

Cytotoxicity Assays

LDH Assay

The Cyquant™ LDH Cytotoxicity Assay (Invitrogen, lot: 2497551) was used to conduct a cytotoxicity assay (**Fig. 8**). Transduced mouse T cells and B16-muc16CD cells were co-cultured at effector-to-target ratios (E:T) for LDH assays since the tumor line did not express luciferase. Mouse CAR T and tumor cells were counted using a BioRad automated cell counter and co-cultured in a 96-well plate in E:T ratios of 1:1, 1:3, 1:10, and 1:30 (**Fig.9**). Each condition had three replicates and the LDH assay also included a minimum and maximum control. At the 48-hour time point, 10µL of tween was used to lyse tumor cells for the maximum control. After incubating for 30 minutes, a substrate stock solution (600µL assay buffer and 11.4 mL diH_2O) was prepared and 50µL of the sample was mixed with the solution in a 96-well flat-bottom plate and incubated for 30 minutes. 50µL of stop solution was mixed with each sample and then measured for absorbance at two wavelengths: 490 nm and 680 nm. The 680 nm wavelength is measured for background reading and subtracted when analyzing. The 96-well flat-bottom plate was read using the Biotek Synergy Microplate Reader and analyzed using Graphpad-Prism. The following formula was used to calculate % cytotoxicity.

$$\text{Cytotoxicity} = \frac{\left(A_{490}\left[\text{Experiment}\right] - A_{490}\left[\text{Low control}\right]\right)}{\left(A_{490}\left[\text{High control}\right] - A_{490}\left[\text{Low control}\right]\right)} \times 100$$

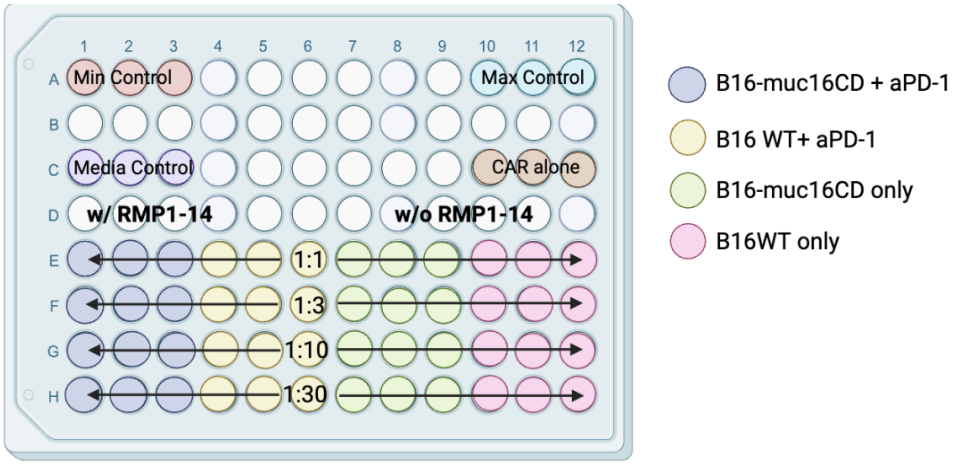

Fig. 9 | LDH Assay Setup for anti-Muc16CD CAR against B16-muc16 tumor cells. Four different effector to target ratios were used and mouse anti-PD-1 (RMP1-14) was also added as a condition. A maximum lysis control is needed to subtract the tumor cells lysed from the total cells lysed. A minimum control is also needed for the formula to subtract from total tumor. Conditions are as follows: 4H11 CAR+B16 WT, 4H11 CAR+B16-Muc16CD, 4H11 CAR+B16WT+aPD-1, 4H11 CAR+B16-Muc16CD+aPD-1.

Cytokine and Degranulation Assay (IFN-g, Granzyme B, CD107a)

Mouse CAR T cells and Muc16CD+ tumor cells were co-cultured at an E:T ratio of 1:3 for 48 hours. GolgiStop (0.5µL/mL) was added at the 20-hour time point for optimal cytokine staining. At the 24-hour time point, cells were collected and fixed and permeabilized with a BD Cytofix/Cytoperm Kit (BD Biosciences, BD 554714). Intracellular staining was performed with αCAR-APC (Biolegend,), αIFN-g-PE (Biolegend,), αGranzymeB-Pe-Cy5 (Biolegend,), and αCD107a-PerCP-Cy5.5 (Biolegend,). Cytokine levels and degranulation levels were quantified using median fluorescence intensity (MFI) and % positive population of the cells from intracellular staining flow cytometry.

Activation and Proliferation Assay (CD69 and CFSE)

Mouse CAR T cells and Muc16CD+ tumor cells were co-cultured at an E:T ratio of 1:3 for 24 hours. At the 20-hour time point, GolgiStop (0.5µL/mL) was added for optimal cytokine staining. At the 24-hour time point, cells were collected and fixed and permeabilized

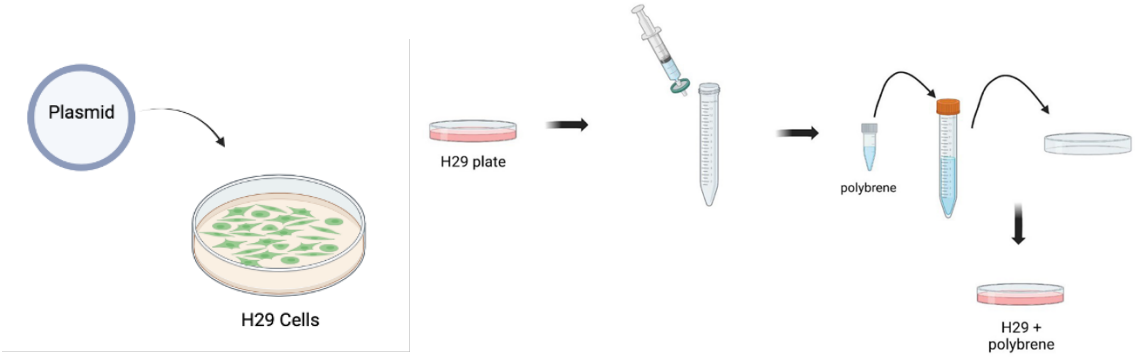

Made with Biorender

Fig.10 | Transfection and Transduction of construct and packaging cells. Transfection involves transiently introducing DNA plasmid into cells. Since H29 cells only last for three days, transduction is conducted with the H29 cells to express the plasmid in a stably-producing packaging cell line (Phoenix Eco Cells).

(BD Biosciences, BD 554714). Intracellular staining was performed with αCD69-(BD Biosciences, cat. 55809), αCFSE (Invitrogen, lot. 2266587), and αCAR-APC (Biolegend). Activation and proliferation markers were quantified using median fluorescence intensity (MFI) on flow cytometry. The gate for CFSE+ populations were drawn based on the fresh CFSE samples, instead of using the unstimulated conditions as a reference for the gate, and the CD69+ populations were drawn based on unstimulated conditions as a reference.

Tumor Injection and Imaging

All mouse study protocols were approved by IACUC. Twelve C57BL/6 mice were engrafted with 1×10^5 YUMM-Muc16CD-GFPffluc tumor in 200µL PBS. Each mouse was subcutaneously (SQ) injected five days prior to CAR T cell and αPD-1 treatment. On the first day of treatment, the mice were injected intraperitoneally (IP) with D-luciferin (98mM/mouse) and

then imaged with the IVIS imaging system. The mice were randomized based on the similar average luminescence between each group. All mice were imaged once a week and injected with D-luciferin (98mM/mouse) every time they were imaged. Mice in the treatment groups were then injected with 4×10^6 CAR T cells and αPD-1 (200μg/200μL) respectively. Three days after the first treatment, mice in the treatment groups were treated with αPD-1 (200μg/200μL) and three days after that with αPD-1 (200μg/200μL) once more.

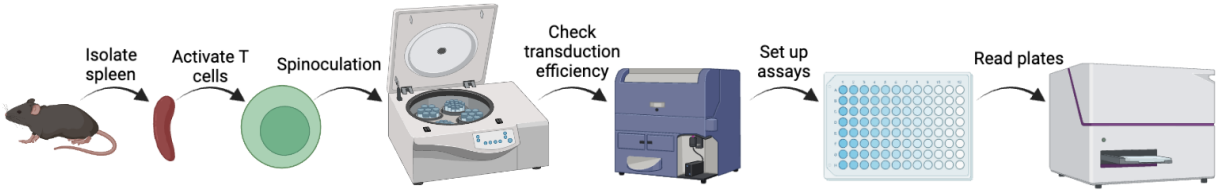

Fig.11 | Transducing Mouse T cells with CAR packaging cells. This procedure is a five-day protocol with Day 1 starting with isolating splenocytes from the C57BL/6 mice. Once T cells are activated, Days 2 and 3 involve spinning the cells with CAR packaging cells on retronectin plates for one hour. Day 4 the T cells rest and are fed IL-2. And Day 5, transduction efficiency is read and respective assays are set up.

Measuring tumors and evaluating tumor burden scores

According to IACUC protocol, mice were required to be sacked if the tumor was no bigger than 18 mm on each side. Thus, tumors were measured with calipers and tumor endpoint was at a volume of 2000 mm^3. Mice were sacked if tumors reached endpoint or ulcerated.

Statistical Analysis

GraphPad Prism was used to run ANOVA statistical testing on results from the CD107a and granzyme B assays. Graphpad Prism was also used for p values of the survival curves to compare each experimental group. All data were graphed through GraphPad Prism as well.

Results

Results

Retrovirally transduced YUMM cells express Muc16CD, GFP, and luciferase.

To test combination therapy of CAR T cell and anti-PD-1 therapy in a clinically relevant mouse melanoma model, the Yale University Mouse Melanoma (YUMM) cell line was transduced with Muc16CD-GFP-firefly-Luciferase (Muc16CD-GFP-ffluc) fusion gene. Following retroviral transduction, the YUMM tumor cells expressed Muc16CD at 60.4%. GFP was also retrovirally transduced with the YUMM cells and after flow analysis, GFP expression was at 56.9% (**Fig. 12 a,b).** To ensure that the YUMM-Muc16CD cells continuously express Muc16CD and GFP, the tumor cells were FACS sorted to 99% expression of Muc16CD (**Supp. Fig. 1**). Finally, luciferase was transduced to the YUMM cells to use for bioluminescence imaging for in vivo and in vitro studies. To validate the luciferase expression, luciferin was added to 10,000 and 50,000 YUMM cells and after 30 minutes, luciferase was shown to be expressed (**Fig.12c**).

Fig. 12 | a. Muc16CD expression of transduced YUMM cells. b. GFP expression of transduced YUMM cells. c. Luciferase expression on 10,000 and 50,000 transduced YUMM cells with media as the negative control. All cells and media were plated in a 96-well plate and then read on a Biotek plate reader.

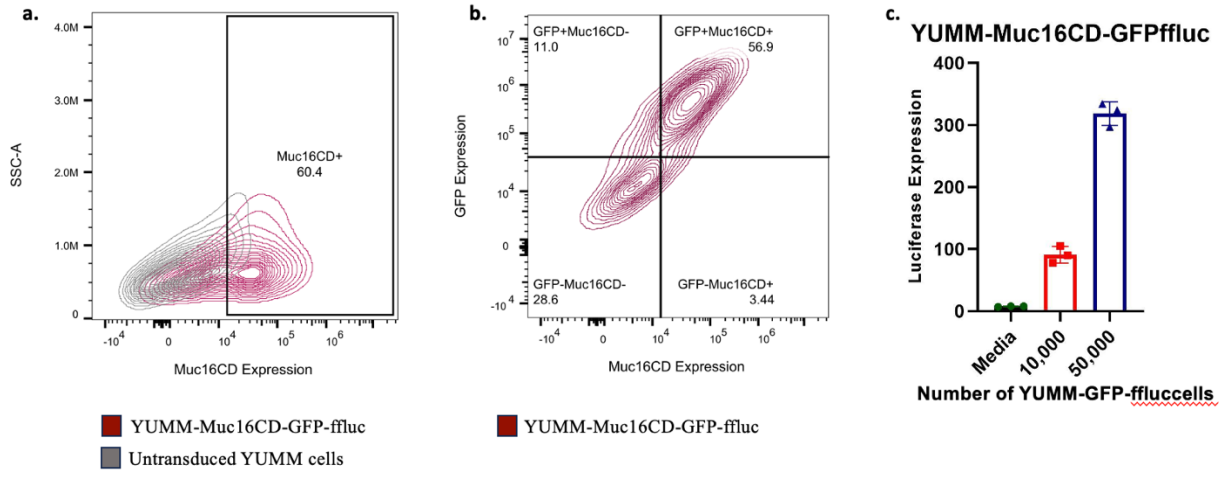

Exposure to IFN-gamma leads to the upregulation of PD-L1 on YUMM Muc16CD-GFPffLuc cells. Upon antigen stimulation, T cells will release IFN-γ that in turn, upregulates PD-L1 on tumor cells (**Fig. 13a**). To confirm this, YUMM-Muc16CD-GFPffluc were cultured with increasing concentrations of 0 ng, 5 ng, and 20 ng of IFN-γ. At 24 hours, flow cytometry analysis reveals that an upregulation of PD-L1 occurs with treatment of 5 ng and 20 ng of IFN-γ (**Fig. 13b**) confirming that the YUMM-Muc16CD-GFPffluc cell line is a good candidate for anti-PD-1 treatment.

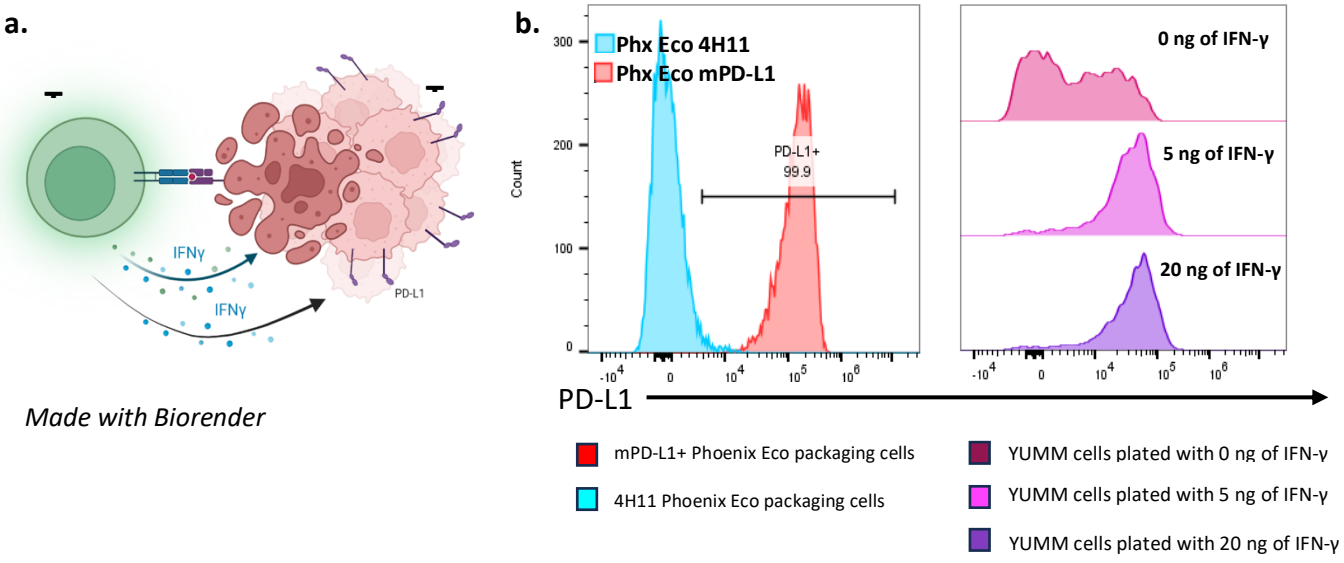

Figure 13 | a. Diagram of when T cells release IFN-γ, PD-L1 expression upregulates on cancer cells. b. YUMM-Muc16CD-GFPffluc cells in different concentrations of IFN-γ.

Mouse T cells can be retrovirally transduced to express anti-Muc16CD CAR.

To test the antitumor efficacy of CAR T cell therapy, we generated the anti-Muc16CD (4H11)-28z CAR.[46] The anti-Muc16CD gene was cloned into a SFG gamma-retroviral vector. The 4H11-28z CAR was designed with variable heavy and light chain sequences from the anti-Muc16CD scFv connected by a G4S linker. The CD28 transmembrane followed the 4H11 scFv and intracellularly, the CD28 and CD3ζ were the signaling domains of the CAR to create a second-generation CAR. To express the CAR construct, retroviral transduction of the construct plasmid

and Phoenix Eco packaging cells was conducted. After transduction, phoenix eco packaging cells had a 99% expression of anti-Muc16CD CAR (**Fig.14a**). Mouse spleens isolated from C57BL/6 mice were used to transduce the CAR packaging cells with mouse T cells. After transducing the mouse T cells, for *in vitro* and *in vivo* experiments, CAR expression on mouse T cells would be up to 54.2% (Fig. 15a.) while overall range would be from 20%-55% (**Fig.16a**) and the viability of the T cells could range from 40%-65% for all experiments (**Fig.16b**).

Figure 14 | a. Transduction efficiency of Phoenix Eco packaging cells of anti-Muc16CD construct. b. Transduction efficiency of anti-Muc16CD+ mouse CAR T cells.

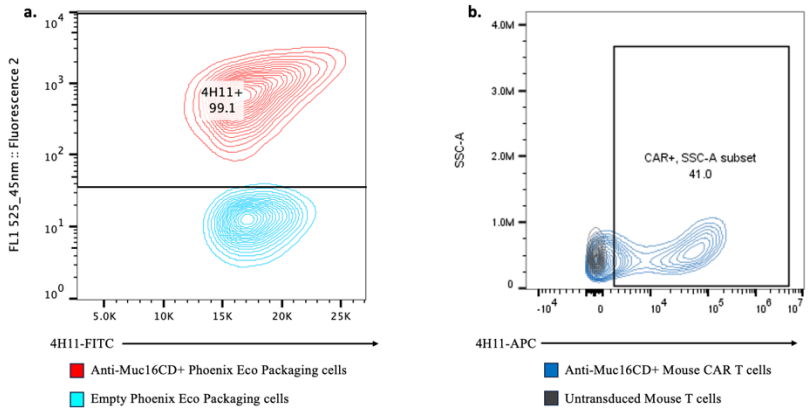

Fig. 15 | a. Flow panels of gating strategy for CAR-positive mouse T cells. b. Transduction efficiency of mouse CAR T cells.

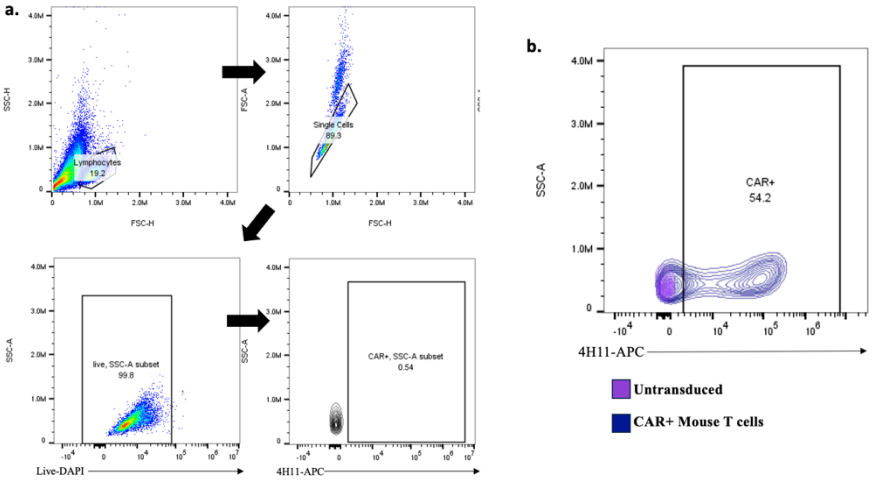

Fig. 16| a. Average transduction efficiency of anti-Muc16CD CAR T cells. b. Average viability of mouse CAR T cells.

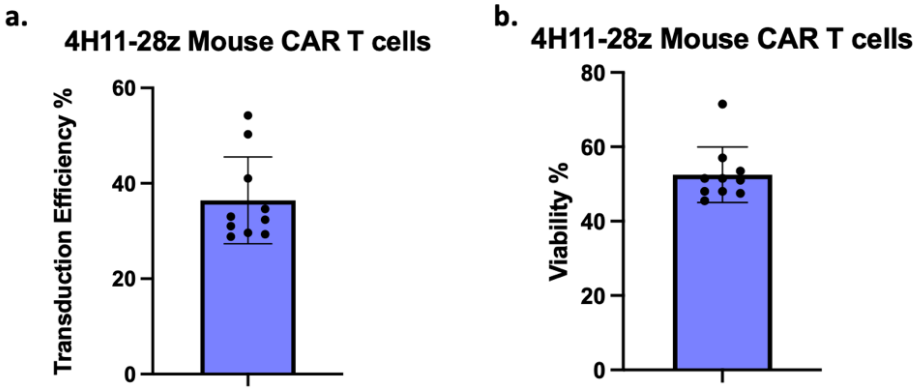

Anti-Muc16CD CAR show specific killing to Muc16CD+ tumor cells.

To validate the CAR construct, we had to determine CAR functionality. First, we assessed cytotoxic capability of 4H11-28z CAR T cells against Muc16CD+ tumor cells. An LDH assay was setup to test the cytotoxicity of the 4H11-28z CAR T cells. Compared to tumor cells that did not express Muc16CD, tumor cells that overexpressed Muc16CD observed a higher percentage of killing by the 4H11-28z CAR overall **(Fig. 17).** Exogenous mouse anti-PD-1 (RMP1-14) was also added as a condition to the cytotoxicity assays. However, there were insignificant differences between the CAR alone condition and CAR+RMP1-14 antibody condition for the percent lysis (**Fig. 17**).

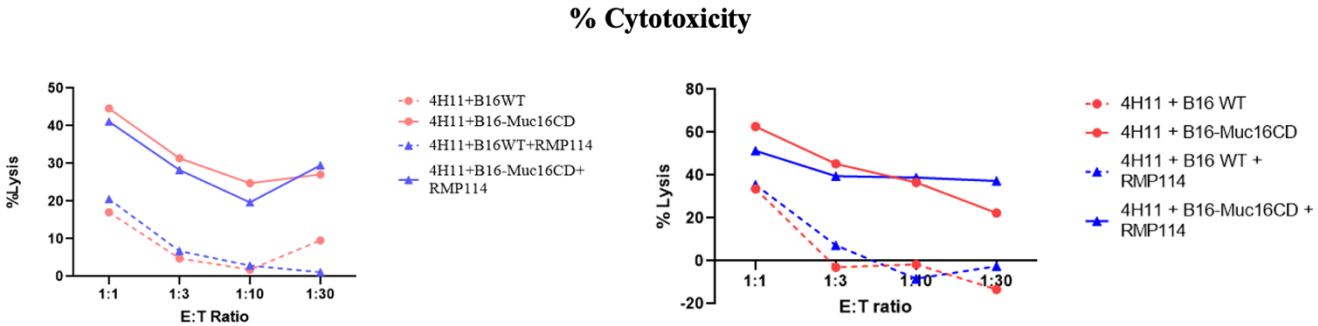

Fig. 17| 4H11-28z CAR was more cytotoxic to Muc16CD+ tumor cells than Muc16CD- cells. The four conditions are depicted in the LDH assay setup (Fig. 9). Overall, the anti-Muc16CD (4H11) CAR shows specific killing to Muc16CD+ tumors. There were no significant differences observed between conditions with RMP1-14 and without RMP1-14.

Anti-Muc16CD CAR shows elevated expression of degranulation, activation, and proliferation markers.

To further test the 4H11-28z functionality, degranulation, activation, and proliferation were tested. 4H11-28z CAR T cells were stimulated with YUMM-Muc16CD-GFP-ffluc cells at an effector to target ratio of 1:3 for 24 hours for the CD107a, IFN-g, granzyme B, and CD69 assays. Additionally, stimulated CAR T cells were cultured with and without RMP1-14 anti-mouse PD-1 antibody totaling the setup to have three conditions per assay. After 24 hours, flow analysis reveals that stimulated CAR T cells demonstrated higher levels and obvious shifts of granzyme B and CD107a compared to unstimulated CAR T cells (**Fig. 18b,c**). Further analysis

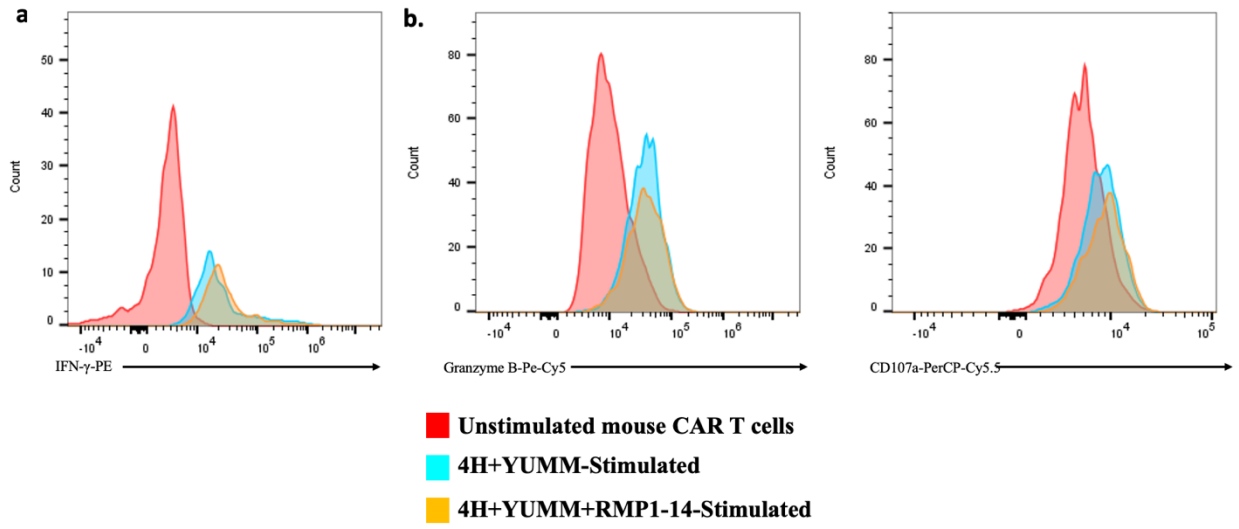

Fig. 18 | Cytokine and degranulation factors were tested on stimulated and unstimulated CAR T cells. CAR T cells were co-cultured with YUMM-Muc16CD-GFPffluc cells to stimulate CAR T cells. a. Flow analysis of IFN-γ on stimulated and unstimulated mouse CAR T cells. b. Flow analysis of CD107a and granzyme B expression on stimulated and unstimulated mouse CAR T cells. Overall, data shows clear shifts of stimulated CAR T cells from the unstimulated CAR T cells indicating that CAR T cells are being activated and show increased cytotoxic capability in the presence of tumor.

with the median fluorescence intensity (MFI) reveals that for granzyme B, there was a significant difference between unstimulated and stimulated for both CAR and CAR + RMP1-14 with a p=0.01 between unstimulated CAR and CAR T cell only conditions and p=0.02 between unstimulated CAR and CAR+RMP1-14 conditions (**Fig.19c**). There was no significance between the two

stimulated conditions. While CD107a levels appeared elevated on flow analysis, there was no significant difference between unstimulated and stimulated CAR T cells with a p=0.37 between unstimulated CAR and stimulated conditions (**Fig. 19b**). However, the MFI still confirms that there were shifts between the unstimulated and stimulated CAR conditions, indicating that there was an increase of CD107a expression in the stimulated CAR conditions (**Fig. 19b**).

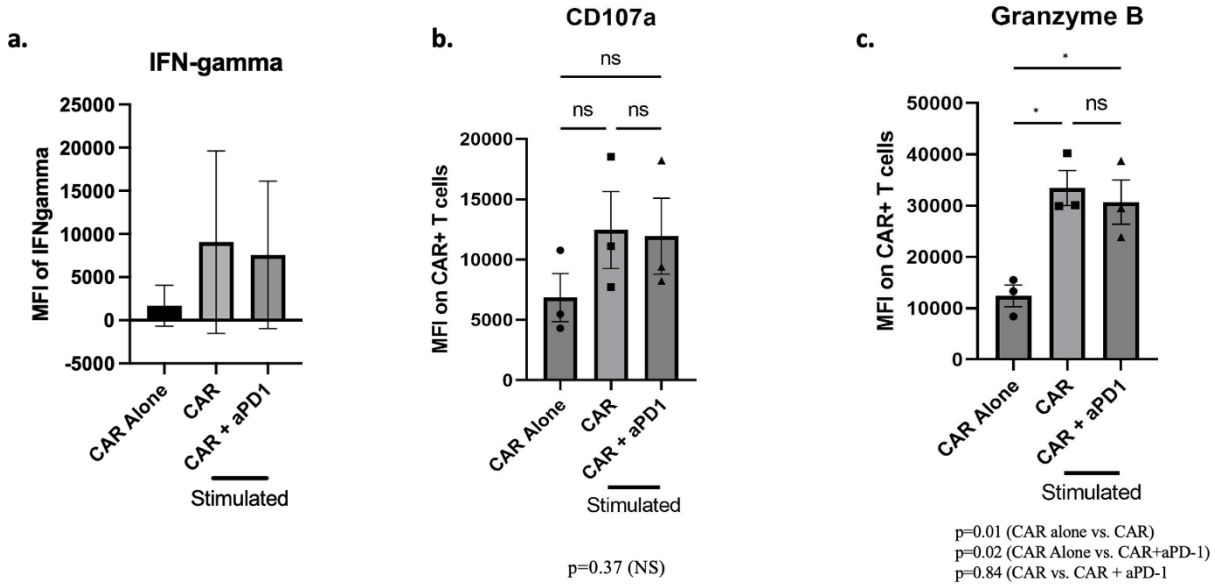

Fig. 19 | Degranulation and activation factors were tested on stimulated and unstimulated CAR T cells. CAR T cells were co-cultured with YUMM-Muc16CD-GFPffluc cells. Data from flow is being depicted with median fluorescence intensity values based off the CAR-positive gate from Fig. 18. a. IFN-g MFI values with an n=2. b. CD107a average MFI on CAR T cells, stimulated and unstimulated. Stimulated CAR conditions were not significant from the unstimulated CAR T cells. c. Granzyme average MFI on stimulated and unstimulated CAR T cells. Both stimulated conditions were significant from the unstimulated CAR T cells. Granzyme B had significant differences between unstimulated 4H11-28z CAR condition and stimulated 4H11-28z CAR condition (p=0.01) as well as unstimulated CAR and stimulated CAR with mouse aPD-1 (p=0.02). CD107a showed no significant differences however, definite shifts of MFI values were observed between the unstimulated and stimulated CAR T cells. Preliminary data of IFN-γ (n=2) **also showed elevated IFN-γ levels for stimulated CAR T cells versus the unstimulated CAR T cells.**

Preliminary flow data shows that between unstimulated and stimulated CAR conditions, there was a definite increase in IFN-γ levels (**Fig. 18a**). Further analysis of the MFI values confirms that IFN-γ is being released when mouse CAR T cells are stimulated (**Fig. 19a**).

Preliminary results of the CD69 activation assay reinforces that stimulated 4H11-28z mouse CAR T cells have higher levels of CD69 expression compared to the unstimulated 4H11-

28z mouse CAR T cells (**Fig. 20b**). For CAR+ mouse T cells, CD69 positive population for the stimulated conditions with and without RMP1-14 were 86.2% and 67.7% respectively (**Fig.20c**). Analysis of the MFI values confirms these results in the stimulated CAR conditions indicating mouse CAR T cells are activated in the presence of tumor while the unstimulated mouse CAR T cells are considerably less activated (**Fig. 20d**).

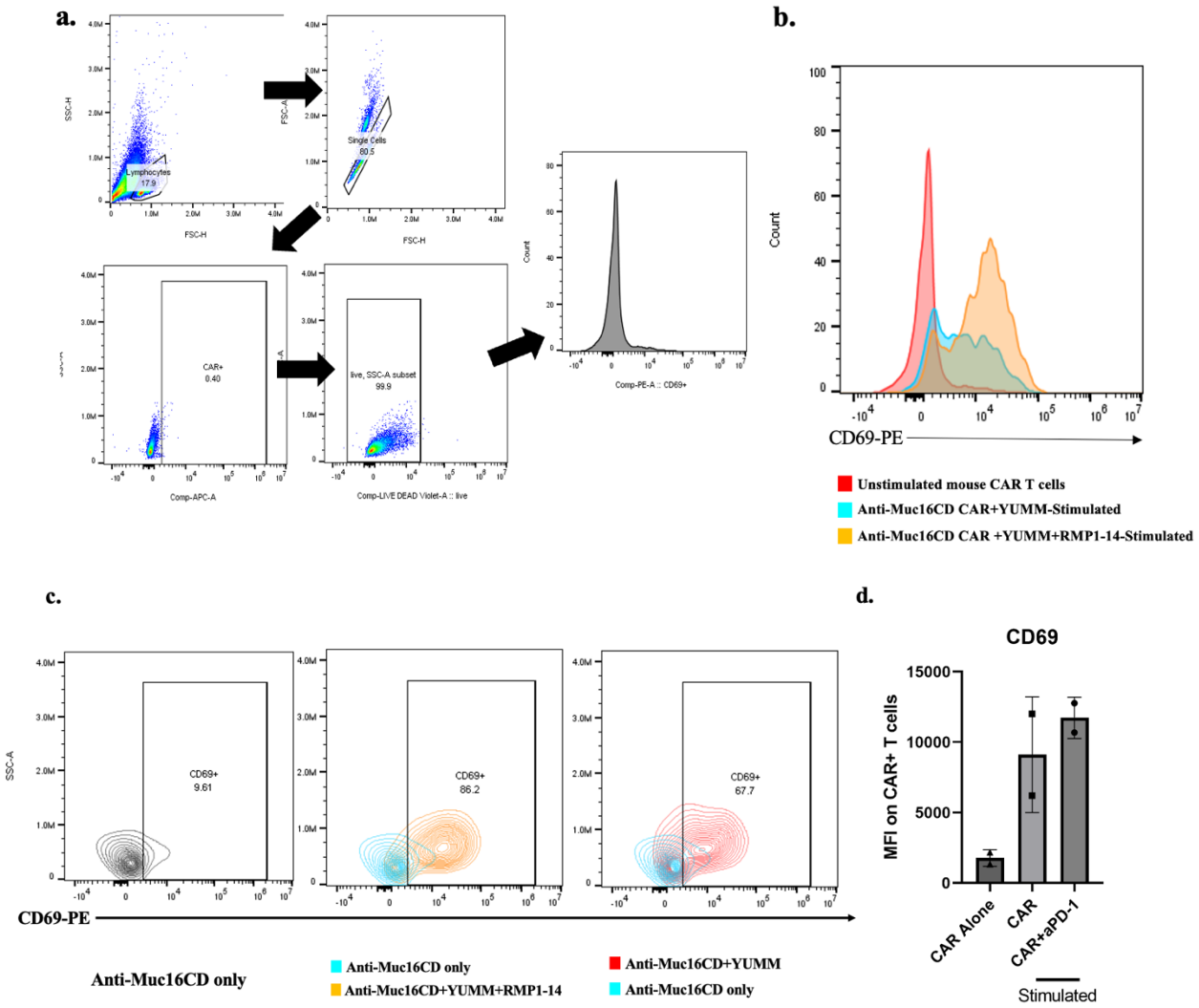

Fig. 20 | Preliminary data of activation of mouse CAR T cells between unstimulated and stimulated conditions. . To avoid the CAR recycling phenomenon,[72] CAR was stained intracellularly while for CD69, surface staining was conducted. a. Gating strategy of flow analysis of CD69 assay b. Stimulated mouse CAR T cells shifts to display increased CD69 expression compared to unstimulated cells. Median fluorescence intensity of stimulated

and unstimulated CAR T cells. MFI values reveal that CAR T cells co-cultured with YUMM-Muc16CD-GFP-ffluc were activated compared to CAR T cells cultured without YUMM-Muc16CD-GFP-ffluc.

For proliferation assay, the CFSE was used as a marker and the assay had a 24 hours and 48 hours setup. and the 4H11-28z only without tumor (unstimulated), 4H11-28z with tumor and 4H11-28z+anti-PD-1 with tumor (stimulated) conditions were setup at 24 hours and 48 hours respectively. At 24 hours, CFSE expression for stimulated cells without RMP1-14 was at 53.7% and with RMP1-14 was at 63.9% whereas unstimulated cells were at 29.5% (**Fig. 21b**). At 48 hours, flow analysis shows that CFSE expression for the stimulated cells without RMP1-14 was 94.3% and with RMP1-14 was at 95.6% whereas unstimulated cells had 19.4% CFSE expression (**Fig. 21c**). Further analysis of the CD8+ CAR T cells from the CFSE positive population reveals that there were 78.6% and 74.4% CD8+ CAR T cells proliferating in the stimulated conditions for the 48-hr. assay and 34.5% and 26.6% CD8+ CAR T cells in the stimulated conditions for the 24-hr. assay (**Fig. 21d,e**). Thus, preliminary data indicates that 4H11-28z mouse CAR T cells were able to proliferate post retroviral transduction in the presence of antigen-presenting YUMM cells, especially at the 48-hr. timepoint.

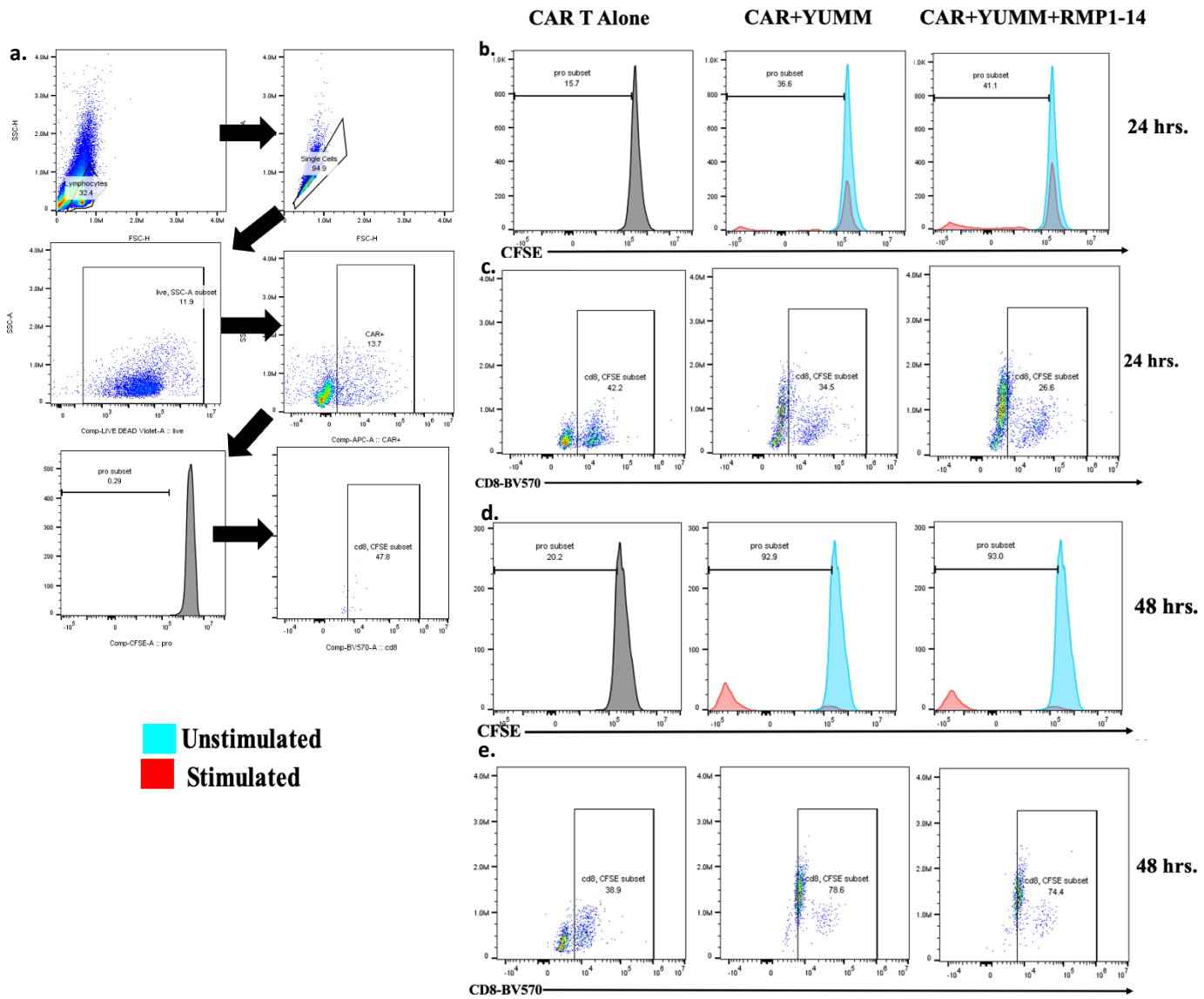

Fig. 21 | Preliminary data of proliferation markers on unstimulated and stimulated mouse CAR T cells. CAR-positive staining was done intracellularly to avoid CAR recycling[72] a. Gating strategy of flow analysis of CFSE assay. The gate was drawn based on fresh CFSE sample. From the fresh CFSE sample, we wanted to see how many CD8+ T cells came from the CFSE positive population, so we gated out CD8+ T cells from there. b. Stimulated mouse CAR T cells shifts to display increased CFSE expression compared to unstimulated cells at 24 hours. c. At 24 hrs, the CD8+ T cell population was gated from the CFSE+ population. d. Stimulated mouse CAR T cells shifts to display increased CFSE expression compared to unstimulated cells at 48 hours. e. At 48 hrs, the CD8+ T cell population was gated from the CFSE+ population. Overall, data depicts that CD8+CAR T cells at 48 hrs. have increased proliferation when stimulated with tumor and over time post five-day mouse CAR T cell transduction.

CAR T cell treatment group shows prolonged survival over the combination treatment group in vivo.

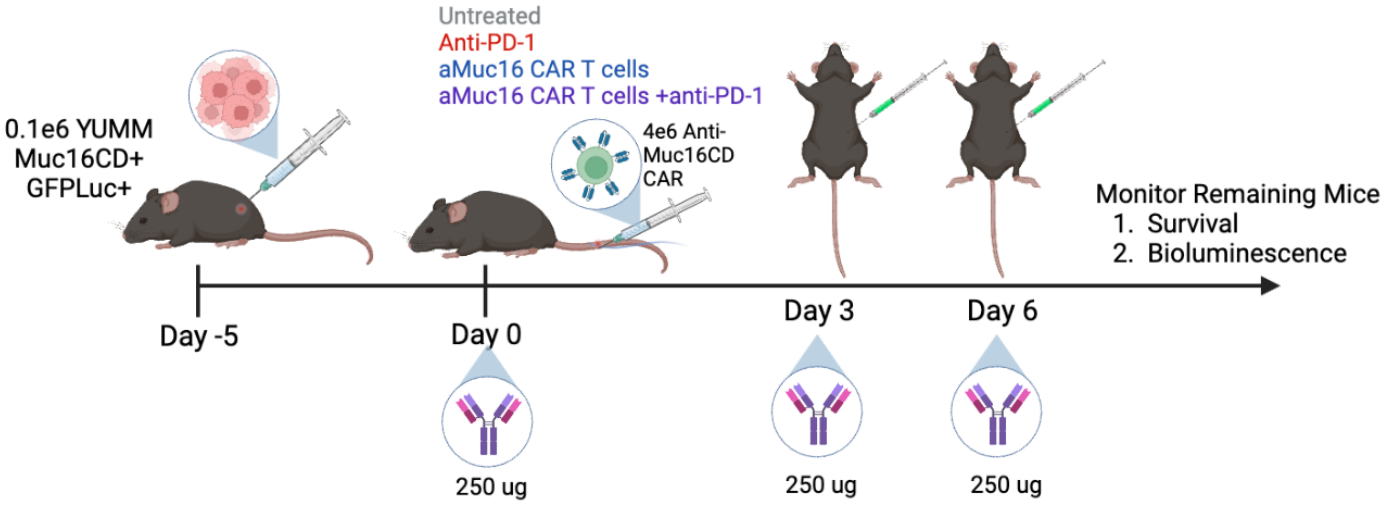

Fig. 22 | In vivo experiment timeline. Mice were treated five days after inoculating mice with YUMM-Muc16CD-GFPffluc tumor. After the last anti-PD-1 treatment, mice were monitored for survival through measuring tumor with calipers twice a week and bioluminescence imaging once a week.

We tested the anti-tumor efficacy of CAR T cell and anti-PD-1 treatment in vivo by inoculating C57BL/6 mice (n=12) with 1×10^5 YUMM-Muc16CD-GFP-ffluc cells each subcutaneously. Tumor-bearing mice were treated five days later with 4×10^6 anti-Muc16CD CAR T cells injected intravenously along with anti-PD-1 to the respective treatment groups. One additional treatment of anti-PD-1 was administered post CAR T cell inoculation and one final anti-PD-1 treatment was administered post the second anti-PD-1 infusion. Tumor burden was measured by bioluminescence imaging weekly and measuring tumor volume biweekly. A few mice had tumors that did not show up on images because the black fur of the mice could have hindered the system from capturing the luminescence of the tumor (**Fig. 23a,b**). Even if some mice did not display bioluminescence on the imaging system, those mice had palpable tumor and were still able to have measurable tumor by using calipers.

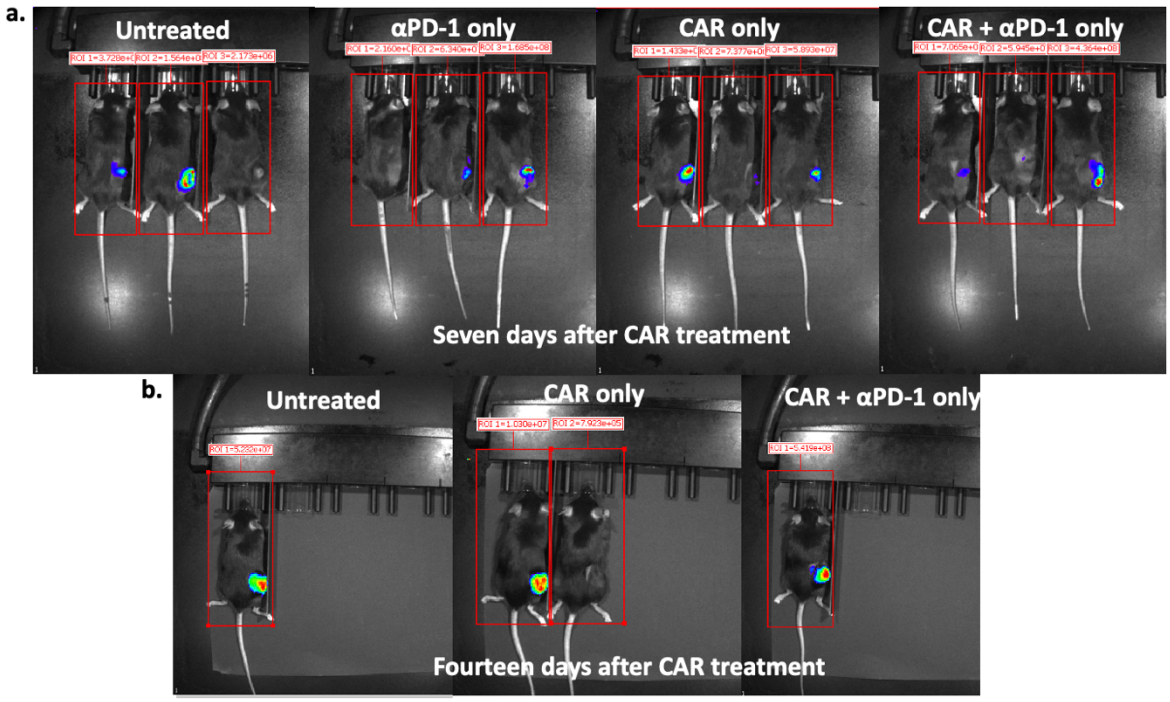

Fig. 23 | Bioluminescence imaging of mice after CAR treatment. We randomized the mice based on bioluminescence imaging into four conditions: untreated (n=3), anti-PD-1 (RMP1-14) only (n=3), CAR T cell (n=3), and combination of CAR and anti-PD-1 (n=3) a. Imaging seven days post CAR treatment. b. Imaging fourteen days post CAR treatment.

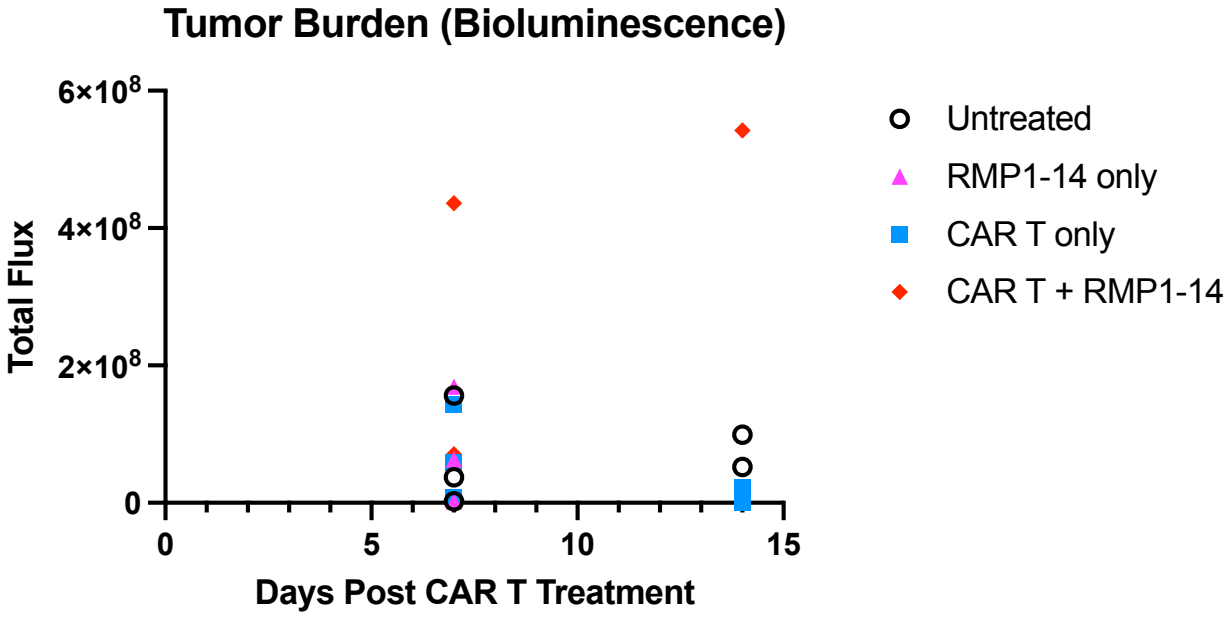

Fig. 24 | Graph depicting tumor burden based on bioluminescence imaging. The y-axis is based on total flux with a 1.2 scope reading.

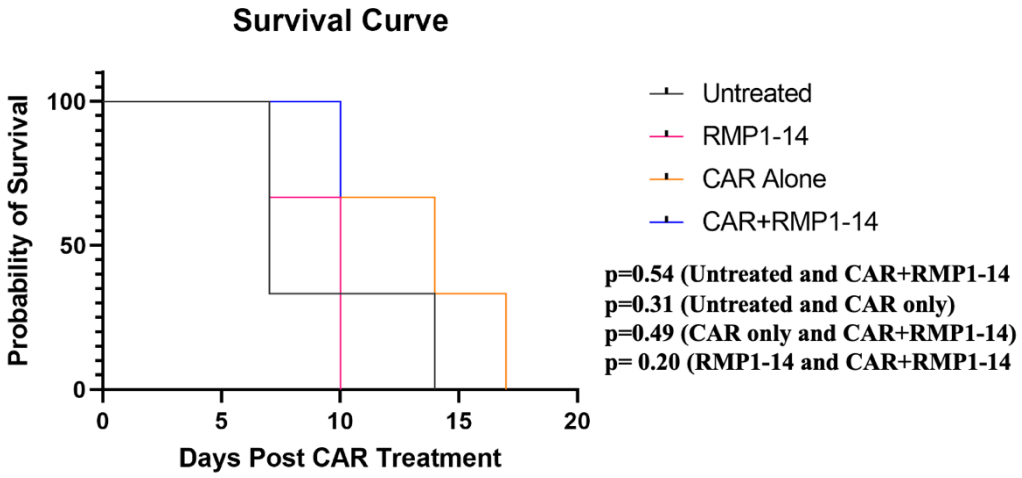

Fig. 25 | Survival Curve of *in vivo* study. There were four conditions with n=3 mice in each group. The groups are as follows: untreated, aPD-1 only, anti-Muc16CD CAR T cell only, and anti-Muc16CD CAR + aPD-1. The final mouse reached endpoint on Day 17. Kaplan-Meier survival analysis was conducted for this study. There were no significant differences observed between any of the treatment groups and untreated group.

Seven days after initial combination treatment, all mice were imaged and upon inspection, a few mice displayed ulceration at the tumor site. All groups except for the CAR and anti-PD-1 treatment group had at least one ulcerated tumor which led to sacking the mice. On Day 10 post-CAR and antibody treatment, all mice from the anti-PD-1 treatment group were sacked due to ulcerated tumors (**Fig. 24**). Two mice from combination treatment group were also sacked due to tumors growing to endpoint (**Fig. 24, 25**). The last untreated mouse was sacked at 14 days post CAR treatment and the final mice from the CAR T cell only treatment was sacked at 17 days thus concluding the *in vivo* study at 21 days total starting when tumors were injected (**Fig. 24**). One mouse from the CAR T cell only treatment group had the slowest tumor growth progression over the untreated and treatment groups (**Fig. 25,26**). The combination treatment group had all three mice until day 10, when one mouse was sacked due to an ulcerated tumor (**Fig. 24**). There were insignificant differences between the treatment groups and untreated group.

Fig. 26 | Each individual mouse tumor growth progression from four conditions: untreated, RMP1-14 only, 4H11 CAR T cell only, and combination conditions.

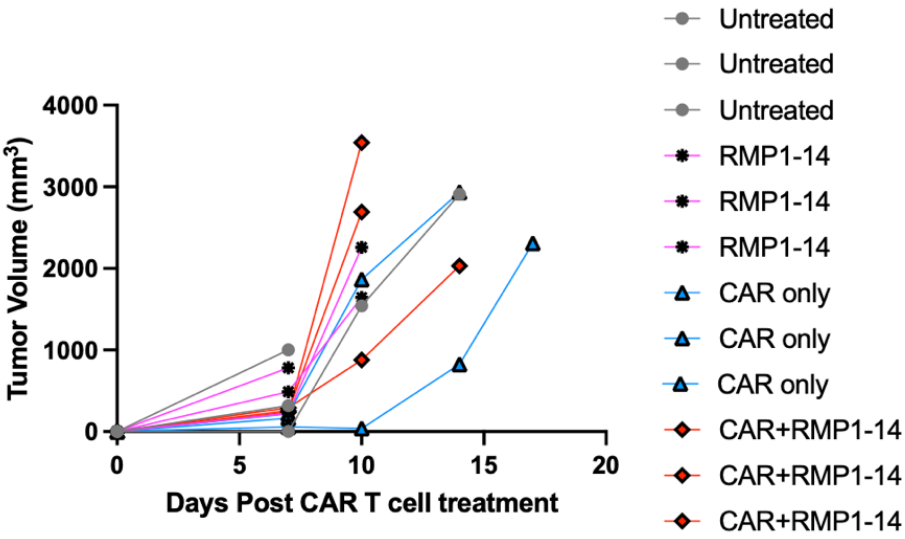

Future Directions

Future Directions

For *in vitro* studies used to validate the CAR functionality, 1:3 ratios were the optimal co-culturing effector to target ratios to effectively stimulate mouse CAR T cells. For future studies, further assays involving CD107a should be optimized. CD107a is very transient and thus, very difficult to capture since it goes back and forth between the cell surface and cytosol. Once optimized, the flow curves between unstimulated mouse CAR T cells and stimulated mouse CAR T cells will have a greater shift and difference. For the cytokine assays, IL-2 levels should also be observed between unstimulated and stimulated mouse CAR T cells to further confirm that the CAR's T cell signaling is functioning properly and effectively. The cytotoxicity assay could be optimized as well by using a non-specific CAR as a negative control versus using a non-specific tumor cell and adding in one more ratio as a datapoint to see more in-depth changes between the killing capabilities of the 4H11-28z CAR. The proliferation assay seems to be optimal at 48 hours but, further experiments with the CFSE staining protocol must be conducted to confirm this timepoint. Finally, for the CD69 assay, to ensure that CAR T cells are being stimulated by the Muc16CD+ tumor, it might be best to add another condition with CAR T cells and Muc16CD- tumor. That way we can truly assess and compare if Muc16CD+ tumor is activating more CAR T cells than the Muc16CD- tumor to further test the specificity of the anti-Muc16CD CAR.

Furthermore, the YUMM-Muc16CD-GFP-ffluc cells used for the *in vitro* and *in vivo* experiments should be further optimized. *In vivo*, The YUMM cells prove to be an aggressive and fast-growing model. Even though measurements were taken more frequently (twice a week), the tumor volume for each mouse almost always progressed to endpoint or ulcerated tumor. Perhaps injecting 5×10^4 cells instead of 1×10^5 cells would allow for a more prolonged timeline *in vivo* study. When working with a B16 melanoma model, also known for being an aggressive model,

the Jim Allison group injected 5×10^4 cells and still resulted in a survival curve that overlapped but were able to have a timeline that spanned longer than 50 days.[57] Therefore, injecting even less tumor in future studies should be considered.

For our in vivo study, optimizing the way anti-PD-1 is administered should be considered. In clinic, humans receive antibody treatment consistently that can span up to one year, depending on toxicities.[66] In one *in vivo* study, mice were injected with B16 tumors and had multiple treatment groups that included an anti-PD-1 only treatment group. 15 rounds of treatment were administered to each treatment group and the anti-PD-1 treatment group's endpoint was at 30 days.[69] In our *in vivo* study, antibody treatment was given when mice were randomized into their respective treatment groups, and then two more times with three days apart from each other for a total of three antibody treatments to the respective groups. Therefore, treating the tumor with more anti-PD-1 can be an option for future *in vivo* studies particularly to see a prolonged survival curve. Furthermore, perhaps the initial antibody treatment should be administered after initial CAR T cell treatment when mice begin to present palpable tumors. One study examines the antitumor efficacy of combination immunotherapy treatments of anti-OX40 and anti-PD-1 by testing the optimal timing to administer anti-PD-1. The study found that sequential combination treatment with PD-1 blockade versus concurrent combination treatment with PD-1 blockade enhanced the antitumor efficacy of the anti-OX40 treatment that was combined with anti-PD-1.[67] Thus, if antibody treatment was given to the mice more than three times for our preclinical studies or was given antibody treatment after initial CAR treatment, perhaps we would be able to distinguish the differences between combination treatment versus the CAR treatment only groups better.

Discussion

Discussion

In this study, we aimed to increase CAR T cell antitumor efficacy against melanoma by combining CAR T cell and ICI therapies thereby addressing both CAR T cell and ICI therapy's limitations. We investigated CAR T cell function by testing its cytotoxic function, cytokine levels, proliferating and activating capabilities against YUMM tumors. We also tested the *in vitro* and *in vivo* characteristics of the YUMM cells that were taken from a GEMM model with a Braf activation and Pten inactivation mutations, mimicking melanoma seen in clinic. In *in vitro* assays, antigen-stimulated CAR T cells displayed an increase in cytokine levels, such as IFN-γ, and degranulation factors, such as CD107a and granzyme B compared to unstimulated CAR T cells. The anti-Muc16CD CAR was also able to specifically kill Muc16CD+ tumors *in vitro* compared to Muc16CD- tumor. And mouse CAR T cells were also more activated and proliferated when cultured with antigen-expressing cells.

While differences were observed between unstimulated and stimulated mouse CAR T cells, insignificant differences were observed between stimulated mouse CAR T cells with RMP1-14 and stimulated mouse CAR T cells without RMP1-14 in *in vitro* assays. However, this was to be expected as monoclonal antibodies engage the endogenous immune cells, which in these experiments only involved mouse T cells. When testing the efficacy for monoclonal antibodies, researchers typically use other immune cells such as NK cells and mononuclear cells as effector cells.[64] Therefore, because the *in vitro* assays do not involve an entire immune system with different types of immune cells, significant differences between the stimulated conditions, with or without antibody, were not expected nor observed. Additionally, the in vitro assays were set up for a short period of time, which might have not given anti-PD-1 enough time to act. Furthermore,

using ex vivo CAR T cells could have impacted conditions as well since ex vivo CAR T cells have poor viability post our five-day mouse T cell transduction procedure.

The characteristics of YUMM cells were further studied in the *in vitro* and *in vivo* experiments. YUMM cells seem to struggle to grow in cell culture. If split in a 1:10 dilution fashion, YUMM cells struggle to proliferate. YUMM cells are also loosely adherent and when killed by CAR T cells in the *in vitro* assays, YUMM cells would easily detach from the surface of the plate. Thus, when plating YUMM cells, it is important to note to plate just enough YUMM cells, so that the cells proliferate and exercise caution when collecting cells for analysis since the YUMMs are loosely adherent to the bottom of the plate. In contrast, in the *in vivo* experiments, the YUMM-Muc16CD-GFP-ffluc cells proved to be an aggressive model as tumors began to ulcerate at day 7 post initial CAR and RMP1-14 treatment. Most tumor volumes in each condition reached endpoint at day 10, post initial CAR and RMP1-14 treatment. This is interesting because only 1×10^5 YUMM-Muc16CD-GFP-ffluc cells were injected into each mouse and in cell culture, having fewer cells seems to considerably slow down tumor growth for the YUMM cells. However, in vivo, having as few as 1×10^5 cells allow the YUMM cells to proliferate and sustain itself *in vivo*. Retrovirally transducing the YUMM cells with Muc16CD could have caused the tumor cells to be more oncogenic and progress aggressively in the mice as having an overexpression of Muc16CD is linked to worse progression of tumor in humans.[71]

Because of the aggressive progression of the YUMM-Muc16CD-GFP-ffluc cells in the *in vivo* experiment, the overall timeline of the experiment ended at 17 days, post CAR T cell treatment. Against our hypothesis, the CAR T cell only treatment group had tumor volumes that progressed more slowly than the combination treatment group as well as the RMP1-14 treatment group. Additionally, overall survival for the CAR T cell only treatment was longer than the combination

treatment group. While the *in vivo* study does not support our hypothesis the combination treatment group still showed promising results as all three mice were still alive at day 10, post CAR T cell treatment whereas the CAR T cell only treatment group had at least one mouse sacked before day 10 at day 7, post CAR T cell treatment. Moreover, the combination treatment group was the only group that had the least number of mice with ulcerated tumors that caused only one mouse to be sacked at day 10, post CAR T cell treatment and every other treatment group had at least two mice that were sacked due to ulcerated tumors. Moreover, the anti-PD-1 treatment group were the first group to be sacked before the untreated group. Since the anti-PD-1 treatment group and the combination treatment group did not fare well compared to the CAR T cell only treatment group, further optimization of anti-PD-1 administration should be considered. For the combination treatment group, tumor growth seemed to progress faster than other treatment groups and yet did not observe nearly as many ulcerated tumors as the other condition groups. One explanation for this could be pseudo-progression in melanoma. Pseudo-progression is a phenomenon where tumor growth progression is attributed to lymphocyte infiltration.[70] This occurs in clinic when patients are treated with ICI and see increased tumor burden initially before seeing tumor regression.[70] If pseudo-progression is occurring in the combination treatment group, then ways to score tumor burden must be optimized through IACUC for future *in vivo* studies.

Combination of CAR T cell and ICI treatments is still a work in progress but shows promising results preclinically and in clinical trials. TIL therapy has also been used in combination with ICI therapy and shown clinical benefits. However, for TIL therapy, success of expanding TILs with 50% or less of autologous tumor material diminishes and for some patients, TIL expansion can fail.[65] TILs act in an MHC-dependent manner and are collected from the tumor site.[63] As a result, if enough TILs are not collected from the tumor site, then patients cannot qualify for this

mode of treatment. Even though TILs might be a better option for solid tumors due to broad antigen killing, this characteristic of TILs could increase the chances for side effects as normal cells could also be targeted by TILs during treatment. CAR T cells offer a more applicable option to a variety of patients because it works in an MHC-independent manner since the T cells are engineered to target the specific TAA on the tumor. [59] Thus, once CAR T cells acquire a specific TAA, OTOT toxicities can be limited whereas TIL therapy are more prone to OTOT toxicities since it still involves broad antigen killing.

The question remains on how to safely administer ICI and CAR T cell therapy and how to prevent each therapy's respective toxicities. To combat these toxicities, other ways to genetically modify CAR T cells have been developed. In addition to signaling domains, CARs can be engineered to have "armor" to secrete monoclonal antibodies, scFv's, peptides, etc (**Fig. 2**). Armored CAR T cells could help overcome the suppressive TME by locally delivering anti-PD-1, which could limit OTOT toxicities as well.[60] Secreting 4H11-28z CAR T cells have proven the antitumor efficacy of the 4H11-28z CAR T cell secreting anti-PD-1 scFvs *in vitro* as well as in *in vivo*.[19] This study was also able to demonstrate that anti-PD-1 scFvs stayed locally within the TME, suggesting that secreting CAR T cells could offer the safe administration of checkpoint blockade therapy and limit toxicities related to monoclonal antibody treatments.[19] Other combination treatment options are being studied as well as FDA-approved. For example, CAR T cells secreting PD-L1 was tested in regress renal cell carcinoma and found to reduce T cell exhaustion and enhance CAR T cell function in vivo.[61] Moreover, Opdualag, a combination therapy of anti-PD-1 and anti-Lag3, was recently FDA-approved for metastatic melanoma, following the results of a large clinical trial where patients who had received the combination antibody treatment had experienced longer progression-free survival over the antibody alone

treatment groups.[62] Finally, one study found that dual checkpoint blockade, anti-PD-1 and anti-CTLA-4, in combination with ACT with pmel CD8+ T cells increased the antitumor efficacy of the ACT and no treatment-related toxicities in vivo.[68] The field of immunotherapy is constantly growing and CAR T cell therapy in combination with ICI treatment needs to be further studied and validated in solid tumors.

References

1. "Melanoma Skin Cancer Statistics." *Melanoma Skin Cancer Statistics*, www.cancer.org/cancer/types/melanoma-skin-cancer/about/key-statistics.html. Accessed 1 June 2023.
2. "Melanoma Incidence and Mortality, United States–2012–2016." *Centers for Disease Control and Prevention*, 27 June 2019, www.cdc.gov/cancer/uscs/about/data-briefs/no9-melanoma-incidence-mortality-UnitedStates-2012-2016.htm.
3. Davis LE, Shalin SC, Tackett AJ. Current state of melanoma diagnosis and treatment. Cancer Biol Ther. 2019;20(11):1366-1379. doi: 10.1080/15384047.2019.1640032. Epub 2019 Aug 1. PMID: 31366280; PMCID: PMC6804807.
4. Dossett L.A. (Fellow), Kudchadkar R.R. (Assistant Professor) & Zager J.S. (Director of Regional Therapies, Chair of Graduate Medical Education, Associate Member) (2015) BRAF and MEK inhibition in melanoma, Expert Opinion on Drug Safety, 14:4, 559-570, DOI: 10.1517/14740338.2015.1011618
5. Flaherty, K.T., et al. "Combined BRAF and MEK Inhibition in Melanoma with BRAF V600 Mutations." *New England Journal of Medicine*, vol. 367, no. 18, 2012, pp. 1694–1703, https://doi.org/10.1056/nejmoa1210093.
6. Solit B. David, M.D. and Rosen N. M.D. Ph.D. (2011) Resistance to BRAF Inhibition in Melanomas. N Engl J Med **364**: 772-774. DOI: 10.1056/NEJMcibr1013704
7. "Immune Checkpoint Inhibitors." *National Cancer Institute*, www.cancer.gov/about-cancer/treatment/types/immunotherapy/checkpoint-inhibitors. Accessed 1 June 2023.
8. Darvin P, Toor SM, Sasidharan Nair V, Elkord E. Immune checkpoint inhibitors: recent progress and potential biomarkers. Exp Mol Med. 2018 Dec 13;50(12):1-11. doi: 10.1038/s12276-018-0191-1. PMID: 30546008; PMCID: PMC6292890.
9. Han Y, Liu D, Li L. PD-1/PD-L1 pathway: current researches in cancer. Am J Cancer Res. 2020 Mar 1;10(3):727-742. PMID: 32266087; PMCID: PMC7136921.
10. Ai, L., Xu, A., Xu, J. (2020). Roles of PD-1/PD-L1 Pathway: Signaling, Cancer, and Beyond. In: Xu, J. (eds) Regulation of Cancer Immune Checkpoints. Advances in Experimental Medicine and Biology, vol 1248. Springer, Singapore. https://doi.org/10.1007/978-981-15-3266-5_3
11. Chen, X.; Feng, L.; Huang, Y.; Wu, Y.; Xie, N. Mechanisms and Strategies to Overcome PD-1/PD-L1 Blockade Resistance in Triple-Negative Breast Cancer. *Cancers* **2023**, *15*, 104. https://doi.org/10.3390/cancers15010104
12. Guo L, Zhang H, Chen B. Nivolumab as Programmed Death-1 (PD-1) Inhibitor for Targeted Immunotherapy in Tumor. J Cancer. 2017 Feb 10;8(3):410-416. doi: 10.7150/jca.17144. PMID: 28261342; PMCID: PMC5332892.
13. Brahmer JR, Drake CG, Wollner I, Powderly JD, Picus J, Sharfman WH, Stankevich E, Pons A, Salay TM, McMiller TL, Gilson MM, Wang C, Selby M, Taube JM, Anders R, Chen L, Korman AJ, Pardoll DM, Lowy I, Topalian SL. Phase I study of single-agent anti-programmed death-1 (MDX-1106) in refractory solid tumors: safety, clinical activity, pharmacodynamics, and immunologic correlates. J Clin Oncol. 2010 Jul 1;28(19):3167-75. doi: 10.1200/JCO.2009.26.7609. Epub 2010 Jun 1. Corrected and

republished in: J Clin Oncol. 2023 Feb 1;41(4):715-723. PMID: 20516446; PMCID: PMC4834717

14. "Immunotherapy." *AIM at Melanoma Foundation*, 14 July 2022, www.aimatmelanoma.org/how-melanoma-is-treated/immunotherapy/.
15. Gong J, Chehrazi-Raffle A, Reddi S, Salgia R. Development of PD-1 and PD-L1 inhibitors as a form of cancer immunotherapy: a comprehensive review of registration trials and future considerations. J Immunother Cancer. 2018 Jan 23;6(1):8. doi: 10.1186/s40425-018-0316-z. PMID: 29357948; PMCID: PMC5778665.
16. Vareki, Maleki, S. High and low mutational burden tumors versus immunologically hot and cold tumors and response to immune checkpoint inhibitors. *j. immunotherapy cancer* **6**, 157 (2018). https://doi.org/10.1186/s40425-018-0479-7
17. Dobosz P, Stępień M, Golke A, Dzieciątkowski T. Challenges of the Immunotherapy: Perspectives and Limitations of the Immune Checkpoint Inhibitor Treatment. Int J Mol Sci. 2022 Mar 5;23(5):2847. doi: 10.3390/ijms23052847. PMID: 35269988; PMCID: PMC8910928.
18. Rafiq, S., Hackett, C.S. & Brentjens, R.J. Engineering strategies to overcome the current roadblocks in CAR T cell therapy. *Nat Rev Clin Oncol* 17, 147–167 (2020). https://doi.org/10.1038/s41571-019-0297-y
19. Rafiq, S., Yeku, O., Jackson, H. *et al.* Targeted delivery of a PD-1-blocking scFv by CAR-T cells enhances anti-tumor efficacy *in vivo*. *Nat Biotechnol* **36**, 847–856 (2018). https://doi.org/10.1038/nbt.4195
20. Rohaan, M.W., van den Berg, J.H., Kvistborg, P. *et al.* Adoptive transfer of tumor-infiltrating lymphocytes in melanoma: a viable treatment option. *j. immunotherapy cancer* **6**, 102 (2018). https://doi.org/10.1186/s40425-018-0391-1
21. Rosenberg SA, Packard BS, Aebersold PM, Solomon D, Topalian SL, Toy ST, Simon P, Lotze MT, Yang JC, Seipp CA, et al. Use of tumor-infiltrating lymphocytes and interleukin-2 in the immunotherapy of patients with metastatic melanoma. A preliminary report. N Engl J Med. 1988 Dec 22;319(25):1676-80. doi: 10.1056/NEJM198812223192527. PMID: 3264384.
22. Rosenberg SA, Yang JC, Sherry RM, Kammula US, Hughes MS, Phan GQ, Citrin DE, Restifo NP, Robbins PF, Wunderlich JR, Morton KE, Laurencot CM, Steinberg SM, White DE, Dudley ME. Durable complete responses in heavily pretreated patients with metastatic melanoma using T-cell transfer immunotherapy. Clin Cancer Res. 2011 Jul 1;17(13):4550-7. doi: 10.1158/1078-0432.CCR-11-0116. Epub 2011 Apr 15. PMID: 21498393; PMCID: PMC3131487
23. Wu R, Forget MA, Chacon J, Bernatchez C, Haymaker C, Chen JQ, Hwu P, Radvanyi LG. Adoptive T-cell therapy using autologous tumor-infiltrating lymphocytes for metastatic melanoma: current status and future outlook. Cancer J. 2012 Mar-Apr;18(2):160-75. doi: 10.1097/PPO.0b013e31824d4465. PMID: 22453018; PMCID: PMC3315690.
24. Dudley, M.E. Wunderlich, J.R, Shelton, T.E., Even, J., Rosenberg, S.A., 2003. Generation of tumor-infiltrating lymphocyte cultures for use in adoptive transfer therapy for melanoma patients. *J. Immunother*. **26**, 332—342.
25. Taylor B.C. and Balko J.M. 2022. Mechanisms of MHC-I Downregulation and Role in Immunotherapy Response. Front. Immunol. 13. 844-866. doi: 10.3389/fimmu.2022.844866

26. D'Agostino, M., Raje, N. Anti-BCMA CAR T-cell therapy in multiple myeloma: can we do better?. *Leukemia* **34**, 21–34 (2020). https://doi.org/10.1038/s41375-019-0669-4
27. Brudno JN, Maric I, Hartman SD, Rose JJ, Wang M, Lam N, Stetler-Stevenson M, Salem D, Yuan C, Pavletic S, Kanakry JA, Ali SA, Mikkilineni L, Feldman SA, Stroncek DF, Hansen BG, Lawrence J, Patel R, Hakim F, Gress RE, Kochenderfer JN. T Cells Genetically Modified to Express an Anti-B-Cell Maturation Antigen Chimeric Antigen Receptor Cause Remissions of Poor-Prognosis Relapsed Multiple Myeloma. J Clin Oncol. 2018 Aug 1;36(22):2267-2280. doi: 10.1200/JCO.2018.77.8084. Epub 2018 May 29. PMID: 29812997; PMCID: PMC6067798.
28. Cao Y, Lu W, Sun R, Jin X, Cheng L, He X, Wang L, Yuan T, Lyu C and Zhao M (2019) Anti-CD19 Chimeric Antigen Receptor T Cells in Combination With Nivolumab Are Safe and Effective Against Relapsed/Refractory B-Cell Non-hodgkin Lymphoma. *Front. Oncol.* 9:767. doi: 10.3389/fonc.2019.00767
29. "University of Pennsylvania's Personalized Cellular Therapy for Leukemia Receives FDA's Breakthrough Therapy Designation." *Penn Medicine*, www.pennmedicine.org/news/news-releases/2014/july/university-of-pennsylvanias-pe. Accessed 31 May 2023.
30. Braendstrup, Peter, *et al*. "The Long Road to the First FDA-Approved Gene Therapy: Chimeric Antigen Receptor T Cells Targeting CD19." *Cytotherapy*, vol. 22, no. 2, 2020, pp. 57–69, https://doi.org/10.1016/j.jcyt.2019.12.004.
31. Schuster, Stephen J., *et al*. "Tisagenlecleucel in Adult Relapsed or Refractory Diffuse Large B-Cell Lymphoma." *New England Journal of Medicine*, vol. 380, no. 1, 2019, pp. 45–56, https://doi.org/10.1056/nejmoa1804980.
32. Locke FL, Ghobadi A, Jacobson CA, Miklos DB, Lekakis LJ, Oluwole OO, Lin Y, Braunschweig I, Hill BT, Timmerman JM, Deol A, Reagan PM, Stiff P, Flinn IW, Farooq U, Goy A, McSweeney PA, Munoz J, Siddiqi T, Chavez JC, Herrera AF, Bartlett NL, Wiezorek JS, Navale L, Xue A, Jiang Y, Bot A, Rossi JM, Kim JJ, Go WY, Neelapu SS. Long-term safety and activity of axicabtagene ciloleucel in refractory large B-cell lymphoma (ZUMA-1): a single-arm, multicentre, phase 1-2 trial. Lancet Oncol. 2019 Jan;20(1):31-42. doi: 10.1016/S1470-2045(18)30864-7. Epub 2018 Dec 2. PMID: 30518502; PMCID: PMC6733402.
33. Cho S-F, Anderson KC and Tai Y-T (2018) Targeting B Cell Maturation Antigen (BCMA) in Multiple Myeloma: Potential Uses of BCMA-Based Immunotherapy. *Front. Immunol.* 9:1821. doi: 10.3389/fimmu.2018.01821
34. Munshi, Nikhil C., et al. "Idecabtagene Vicleucel in Relapsed and Refractory Multiple Myeloma." *New England Journal of Medicine*, vol. 384, no. 8, 2021, pp. 705–716, https://doi.org/10.1056/nejmoa2024850.
35. "U.S. Food and Drug Administration Approves Bristol Myers Squibb's and Bluebird Bio's ABECMA (Idecabtagene Vicleucel), the First Anti-BCMA Car T Cell Therapy for Relapsed or Refractory Multiple Myeloma." *News*, news.bms.com/news/details/2021/U.S.-Food-and-Drug-Administration-Approves-Bristol-Myers-Squibbs-and-bluebird-bios-Abecma-idecabtagene-vicleucel-the-First-Anti-BCMA-CAR-T-Cell-Therapy-for-Relapsed-or-Refractory-Multiple-Myeloma/default.aspx. Accessed 1 June 2023.

36. Soltantoyeh, T.; Akbari, B.; Karimi, A.; Mahmoodi Chalbatani, G.; Ghahri-Saremi, N.; Hadjati, J.; Hamblin, M.R.; Mirzaei, H.R. Chimeric Antigen Receptor (CAR) T Cell Therapy for Metastatic Melanoma: Challenges and Road Ahead. *Cells* **2021**, *10*, 1450. https://doi.org/10.3390/cells10061450
37. Marofi, F., Motavalli, R., Safonov, V.A. *et al.* CAR T cells in solid tumors: challenges and opportunities. *Stem Cell Res Ther* **12**, 81 (2021). https://doi.org/10.1186/s13287-020-02128-1
38. Villanueva J, Herlyn M. Melanoma and the tumor microenvironment. Curr Oncol Rep. 2008 Sep;10(5):439-46. doi: 10.1007/s11912-008-0067-y. PMID: 18706274; PMCID: PMC5662003.
39. Simon, B, Uslu, U. CAR-T cell therapy in melanoma: A future success story?. *Exp Dermatol*. 2018; 27: 1315– 1321. https://doi.org/10.1111/exd.13792
40. Luo, Zhong, *et al*. "Modulating Tumor Physical Microenvironment for Fueling Car-T Cell Therapy." *Advanced Drug Delivery Reviews*, vol. 185, 2022, p. 114301, https://doi.org/10.1016/j.addr.2022.114301.
41. Zhang, X., Zeng, Y., Qu, Q. *et al.* PD-L1 induced by IFN-γ from tumor-associated macrophages via the JAK/STAT3 and PI3K/AKT signaling pathways promoted progression of lung cancer. *Int J Clin Oncol* **22**, 1026–1033 (2017). https://doi.org/10.1007/s10147-017-1161-7
42. Flugel, C.L., Majzner, R.G., Krenciute, G. *et al.* Overcoming on-target, off-tumour toxicity of CAR T cell therapy for solid tumours. *Nat Rev Clin Oncol* **20**, 49–62 (2023). https://doi.org/10.1038/s41571-022-00704-3
43. Thistlethwaite, F.C., Gilham, D.E., Guest, R.D. *et al.* The clinical efficacy of first-generation carcinoembryonic antigen (CEACAM5)-specific CAR T cells is limited by poor persistence and transient pre-conditioning-dependent respiratory toxicity. *Cancer Immunol Immunother* **66**, 1425–1436 (2017). https://doi.org/10.1007/s00262-017-2034-7
44. Spranger, S., Bao, R. & Gajewski, T. Melanoma-intrinsic β-catenin signalling prevents anti-tumour immunity. *Nature* **523**, 231–235 (2015). https://doi.org/10.1038/nature14404
45. Felder M, Kapur A, Gonzalez-Bosquet J, Horibata S, Heintz J, Albrecht R, Fass L, Kaur J, Hu K, Shojaei H, Whelan RJ, Patankar MS. MUC16 (CA125): tumor biomarker to cancer therapy, a work in progress. Mol Cancer. 2014 May 29;13:129. doi: 10.1186/1476-4598-13-129. PMID: 24886523; PMCID: PMC4046138.
46. Chekmasova AA, Rao TD, Nikhamin Y, Park KJ, Levine DA, Spriggs DR, Brentjens RJ. Successful eradication of established peritoneal ovarian tumors in SCID-Beige mice following adoptive transfer of T cells genetically targeted to the MUC16 antigen. Clin Cancer Res. 2010 Jul 15;16(14):3594-606. doi: 10.1158/1078-0432.CCR-10-0192. Epub 2010 Jul 13. PMID: 20628030; PMCID: PMC2907178.
47. Koneru, M., O'Cearbhaill, R., Pendharkar, S. *et al.* A phase I clinical trial of adoptive T cell therapy using IL-12 secreting MUC-16^{ecto} directed chimeric antigen receptors for recurrent ovarian cancer. *J Transl Med* **13**, 102 (2015). https://doi.org/10.1186/s12967-015-0460-x
48. O'Cearbhaill, Roisin Eilish, et al. "A Phase I Clinical Trial of Autologous Chimeric Antigen Receptor (CAR) T Cells Genetically Engineered to Secrete IL-12 and to Target the Muc16ecto Antigen in Patients (PTS) with Muc16ecto+ Recurrent High-Grade Serous

Ovarian Cancer (HGSOC)." *SGO*, 30 Mar. 2020, sgo.confex.com/sgo/2020/meetingapp.cgi/Paper/16374.

49. Wang Q, Yang Y, Yang M, Li X, Chen K. High mutation load, immune-activated microenvironment, favorable outcome, and better immunotherapeutic efficacy in melanoma patients harboring *MUC16*/CA125 mutations. Aging (Albany NY). 2020 Jun 3;12(11):10827-10843. doi: 10.18632/aging.
50. Kverneland AH, Pedersen M, Westergaard MCW, Nielsen M, Borch TH, Olsen LR, Aasbjerg G, Santegoets SJ, van der Burg SH, Milne K, Nelson BH, Met Ö, Donia M, Svane IM. Adoptive cell therapy in combination with checkpoint inhibitors in ovarian cancer. Oncotarget. 2020 Jun 2;11(22):2092-2105. doi: 10.18632/oncotarget.27604. PMID: 32547707; PMCID: PMC7275789.
51. O'Malley D, Lee S, Psyrri A*, et al.* 492 Phase 2 efficacy and safety of autologous tumor-infiltrating lymphocyte (TIL) cell therapy in combination with pembrolizumab in immune checkpoint inhibitor-naïve patients with advanced cancers *Journal for ImmunoTherapy of Cancer* 2021;**9:**doi: 10.1136/jitc-2021-SITC2021.492
52. Adusumilli PS, Zauderer MG, Rivière I, Solomon SB, Rusch VW, O'Cearbhaill RE, Zhu A, Cheema W, Chintala NK, Halton E, Pineda J, Perez-Johnston R, Tan KS, Daly B, Araujo Filho JA, Ngai D, McGee E, Vincent A, Diamonte C, Sauter JL, Modi S, Sikder D, Senechal B, Wang X, Travis WD, Gönen M, Rudin CM, Brentjens RJ, Jones DR, Sadelain M. A Phase I Trial of Regional Mesothelin-Targeted CAR T-cell Therapy in Patients with Malignant Pleural Disease, in Combination with the Anti-PD-1 Agent Pembrolizumab. Cancer Discov. 2021 Nov;11(11):2748-2763. doi: 10.1158/2159-8290.CD-21-0407. Epub 2021 Jul 15. PMID: 34266984; PMCID: PMC8563385.
53. Qi, C., Gong, J., Li, J. *et al.* Claudin18.2-specific CAR T cells in gastrointestinal cancers: phase 1 trial interim results. *Nat Med* **28**, 1189–1198 (2022). https://doi.org/10.1038/s41591-022-01800-8
54. aPD-1-MSLN-CAR T cells for the Treatment of MSLN-positive Advanced Solid Tumors. NCT05373147. 13 May, 2022.
55. Meeth K, Wang JX, Micevic G, Damsky W, Bosenberg MW. The YUMM lines: a series of congenic mouse melanoma cell lines with defined genetic alterations. Pigment Cell Melanoma Res. 2016 Sep;29(5):590-7. doi: 10.1111/pcmr.12498.
56. Alvarez, E. (2011). B16 Murine Melanoma: Historical Perspective on the Development of a Solid Tumor Model. In: Teicher, B. (eds) Tumor Models in Cancer Research. Cancer Drug Discovery and Development. Humana Press, Totowa, NJ. https://doi.org/10.1007/978-1-60761-968-0_4
57. Curran MA, Montalvo W, Yagita H, Allison JP. PD-1 and CTLA-4 combination blockade expands infiltrating T cells and reduces regulatory T and myeloid cells within B16 melanoma tumors. Proc Natl Acad Sci U S A. 2010 Mar 2;107(9):4275-80. doi: 10.1073/pnas.0915174107.
58. "LDH Cytotoxicity Assay." *Creative Bioarray*, www.creative-bioarray.com/ldh-cytotoxicity-assay.htm. Accessed 31 May 2023.
59. Dotti G, Gottschalk S, Savoldo B, Brenner MK. Design and development of therapies using chimeric antigen receptor-expressing T cells. Immunol Rev. 2014 Jan;257(1):107-26. doi: 10.1111/imr.12131. PMID: 24329793; PMCID: PMC3874724.

60. Evans AN, Lin HK, Hossian AKMN, Rafiq S. Using Adoptive Cellular Therapy for Localized Protein Secretion. Cancer J. 2021 Mar-Apr 01;27(2):159-167. doi: 10.1097/PPO.0000000000000510. PMID: 33750076; PMCID: PMC7988838.
61. Suarez ER, Chang de K, Sun J, Sui J, Freeman GJ, Signoretti S, Zhu Q, Marasco WA. Chimeric antigen receptor T cells secreting anti-PD-L1 antibodies more effectively regress renal cell carcinoma in a humanized mouse model. Oncotarget. 2016 Jun 7;7(23):34341-55. doi: 10.18632/oncotarget.9114. PMID: 27145284; PMCID: PMC5085160.
62. "OPDUALAG Approved to Treat Advanced Melanoma." *National Cancer Institute*,www.cancer.gov/news-events/cancer-currents-blog/2022/fda-opdualag-melanoma-lag-3. Accessed 1 June 2023.
63. Housseau, F., Zeliszewski, D., Roy, M., Paradis, V., Richon, S., Ricour, A., Bougaran, J., Prapotnich, D., Vallancien, G., Benoit, G., Desportes, L., Bedossa, P., Hercend, T., Bidart, J.-M. and Bellet, D. (1997), MHC-dependent cytolysis of autologous tumor cells by lymphocytes infiltrating urothelial carcinomas. Int. J. Cancer, 71: 585-594. https://doi.org/10.1002/(SICI)1097-0215(19970516)71:4<585::AID-IJC13>3.0.CO;2-B
64. Golay, Josée, and Martino Introna. "Mechanism of Action of Therapeutic Monoclonal Antibodies: Promises and Pitfalls of in Vitro and in Vivo Assays." *Archives of Biochemistry and Biophysics*, vol. 526, no. 2, 2012, pp. 146–153, https://doi.org/10.1016/j.abb.2012.02.011.
65. Geukes Foppen, M.H., Donia, M., Svane, I.M., Haanen, J.B.A.G., (2015), Tumor-infiltrating lymphocytes for the treatment of metastatic cancer, *Molecular Oncology*, 9, doi: 10.1016/j.molonc.2015.10.018.
66. Banks LB, Sullivan RJ. When is it OK to Stop Anti-Programmed Death 1 Receptor (PD-1) Therapy in Metastatic Melanoma? Am J Clin Dermatol. 2020 Jun;21(3):313-321. doi: 10.1007/s40257-020-00506-2. PMID: 32026236; PMCID: PMC7276295.
67. Messenheimer DJ, Jensen SM, Afentoulis ME, Wegmann KW, Feng Z, Friedman DJ, Gough MJ, Urba WJ, Fox BA. Timing of PD-1 Blockade Is Critical to Effective Combination Immunotherapy with Anti-OX40. Clin Cancer Res. 2017 Oct 15;23(20):6165-6177. doi: 10.1158/1078-0432.CCR-16-2677. Epub 2017 Aug 28. PMID: 28855348; PMCID: PMC5641261.
68. Shi L.Z., Goswami S., Fu T., Guan, B., Chen, J., Xiong L., Zhang J., Tang D.N., Zhang X., Vence L., Blando J., Allison J.P., Collazo R., Gao J., Sharma, P. Blockade of CTLA-4 and PD-1 Enhances Adoptive T-cell Therapy Efficacy in an ICOS-Mediated Manner. *Cancer Immunol Res* 1 November 2019; 7 (11): 1803–1812. https://doi.org/10.1158/2326-6066.CIR-18-0873
69. Quixabeira D.C.A., Cervera-Carrascon V., Santos J.M, Clubb J.H.A., Kudling T.V., Basnet S., Heiniö C., Grönberg-Vähä-Koskela S., Anttila M., Havunen R., Kanerva A. & Hemminki A. (2022) Local therapy with an engineered oncolytic adenovirus enables antitumor response in non-injected melanoma tumors in mice treated with aPD-1, OncoImmunology, 11:1, DOI: 10.1080/2162402X.2022.2028960
70. Simard, J.L., Smith, M. & Chandra, S. Pseudoprogression of Melanoma Brain Metastases. *Curr Oncol Rep* **20**, 91 (2018). https://doi.org/10.1007/s11912-018-0722-x

71. Wang Z, Hou H, Zhang H, Duan X, Li L, Meng L. Effect of *MUC16* mutations on tumor mutation burden and its potential prognostic significance for cutaneous melanoma. Am J Transl Res. 2022 Feb 15;14(2):849-862.
72. Chapman NM, Gottschalk S, Chi H. Preventing Ubiquitination Improves CAR T Cell Therapy via 'CAR Merry-Go-Around'. *Immunity*. Aug 18 2020;53(2):243-245. doi:10.1016/j.immuni.2020.07.023
73. Maio M, Grob JJ, Aamdal S, et al. Five-year survival rates for treatment-naive patients with advanced melanoma who received ipilimumab plus dacarbazine in a phase III trial. *J Clin Oncol.* 2015;33(10):1191–1196.
74. Force J, Salama AK. First-line treatment of metastatic melanoma: role of nivolumab. Immunotargets Ther. 2017 Feb 13;6:1-10. doi: 10.2147/ITT.S110479. PMID: 28243579; PMCID: PMC5315343.

Appendix I: Protocols

Protocol for retroviral transduction

Materials and Reagents:

1. DMEM (10% FBS)
2. Phoenix Eco Packaging Cells (Brentjens Lab)
3. 4H11 SFG retroviral plasmid (Brentjens Lab)
4. H29 cells (Brentjens Lab)
5. CaPO4 Promega Transfection Kit
6. Polybrene

Equipment:

1. Serological pipettes
2. 10 cm dish
3. 15 mL conical tube

Procedure:

1. The day before transfection, plate H29 cells.
2. Using the CaPO4 Promega Kit, add CaCL2 to DNA plasmid and also add HBS while vortexing.
3. Incubate at room temperature for 20 minutes.
4. After incubation, aspirate H29 media and add 1000 uL of transfection mix to cover the H29 plate.
5. Add 8 mL of 10% FBS + DMEM media.
6. The next day, change the media on H29 plate.
7. Check transduction efficiency (should be around 80-90%).
8. For transduction, plate Phoenix Eco packaging cells the day before transduction.
9. Collecting H29 supernatant using a 0.45µM filter.
10. Add polybrene to filtered supernatant (8mg/mL).
11. Aspirate supernatant into empty Phoenix Eco packaging cells plate.
12. Replace media on H29 plate.
13. Repeat for the next day.
14. The final day, let cells rest and replace the media on the plate.
15. The next day, check transduction efficiency.

Protocol for Mouse T cell transduction:

Materials and Reagents:

1. RPMI + 10% FBS + 3% ATOS (Complete Media)

2. Retronectin
3. Concanvalin A (con A) (Millipore Sigma)
4. rIL-2
5. Ethanol
6. PBS
7. Red blood cell lysis buffer

Equipment:

1. Beaker
2. Forceps
3. Scissors
4. Syringe w/o needle
5. 10 cm dish
6. 6-well plate Treated
7. 50 mL tube
8. 70µM cell strainer filter
9. Centrifuge
10. Serological pipettes
11. T75 flasks

Procedure:

1. A day before transduction, change media on 4H11 packaging cells.
2. Sack one mouse and immediately bring into culture hood or keep on ice.
3. Take the mouse and transfer it into the beaker with ethanol.
4. Add PBS into a 10 cm plate.
5. Remove mouse from the ethanol and isolate the spleen from the mouse.
6. Immediately, transfer the spleen into the 10 cm plate.
7. Open the syringe and using the plunger, mash the spleen to release lymphocytes.
8. Using a serological pipette, collect the mashed spleen and lymphocytes and filter it through a 70µM cell strainer into a 50mL tube.
9. Wash the plate two more times with PBS and collect as many cells as possible and filter it into the 50 mL tube.
10. Spin the cells for 10 minutes at 1200 rpm.
11. After aspirating the supernatant, resuspend the pellet in 5 mL of RBC lysis for 5 minutes.
12. Neutralize the RBC lysis with 10 mL of Complete Media.
13. Spin down the cells for 10 minutes at 1200 rpm.
14. Resuspend in 30 mL of complete media with 120 uL of ConA and 30 uL of rIL-2.
15. Transfer cells into a T75 flask.
16. For the next two days, measure out 3e6 cells/well (of 6-well retronectin plate) and spin for 60 minutes at 3200 rpm.
17. After spinning for two days, let the mouse T cells rest and feed rIL-2.
18. The final day check for CAR transduction efficiency and setup for respective assays.

Protocol for Cytokine, CFSE, CD69 Assay

Materials and Reagents:

1. BD Cytofix/Cytoperm Kit (BD Biosciences, BD 554714).

2. mIFN-g-PE (Biolegend, cat. 104507)
3. mCD4-BV750 (Biolegend, cat.100467)
4. mCD8-BV570 (Biolegend, cat. 100740)
5. mCD3-Alexa Fluor700 (Biolegend, cat. 100215)
6. mGranzymeB-Pe/Cyanine 5 (Biolegend, cat. 372225)
7. mCD107a-PerCP/Cyanine5.5 ((Biolegend, cat. 121625)
8. FACS Buffer (2.5% FBS, PBS)
9. PBS
10. RMP1-14 (BioXCell, cat. #BE0146)
11. L/D violet
12. CFSE (Invitrogen, lot. 2266587)
13. CD69 (BD Biosciences, cat. 558091).
14. GolgiStop (BD Biosciences, cat. 51-2092KZ)

Equipment:

1. Centrifuge
2. 12-well plate
3. Micropipettes
4. Chemical hood
5. Facs tubes

Procedure:

1. After transducing mouse T cells with CAR packaging cells, set up co-culture 4H11 CAR with YUMM-Muc16CD-GFP-ffluc with and without RMP1-14 in a 12-well plate.
    a. Also plate 4H11 CAR T cells in a well by itself without tumor.
2. After 24 hours, collect all the cells in facs tubes.
3. Four hours before fixing and perming the cells for intracellular staining, add 0.5 uL of GolgiStop.
4. After GolgiStop, prepare cells for surface staining with surface markers: L/D, mCD3, mCD4, and mCD8.
    a. Wash cells 3x with PBS before staining.
5. Stain with surface markers for 30 minutes.
6. After 30 minutes, fix in 250 uL of fixation buffer for 20 min. Vortex for 30 seconds and then incubate in 4 degrees Celsius.
    a. Put on facs tube caps because of formaldehyde from fixation buffer.
7. After 20 minutes, spin down cells for 3 minutes at 1800 rpm and aspirate the supernatant.
8. *Dilute perm/wash buffer, 1:10 dilution with PBS.
9. In chemical hood, remove fixation buffer and wash with 250 uL of wash/perm buffer.
    a. Vortex for 30 seconds.
    b. Spin down cells.
    c. Repeat one more time.
10. Remove wash/perm buffer and resuspend cells in 500 uL of FACS buffer.
11. Can perform IC staining or store for up to five days in 4 degrees Celsius.
    a. Intracellular staining: CAR (4H11-APC),
12. Once IC staining is done, conduct flow cytometry analysis.

Protocol for in vivo study

Materials and Reagents:

1. PBS
2. RMP1-14 (BioXCell, cat. #BE0146)
3. Dluciferin

Equipment:

1. Syringes
2. Facs tubes
3. Ice
4. BioRad Cell counter
5. Cell counting slides
6. Micropipettes

Procedure:

1. After conducting mouse spleen isolation to generate CAR T cells for treatment, prepare YUMM-Muc16CD-GFP-ffluc cells for inoculation.
2. Count tumor cells 2x using cell counter (BioRad).
    a. Do necessary calculations to get to a concentration of 100,000 cells/200uL.
3. At the mouse facilities, using a syringe, inject 200 uL of resuspended tumor cells subcutaneously.
4. Five days post tumor inoculation, use IVIS imaging system to image for tumor for randomization of mice into 4 conditions: untreated (n=3), aPD-1 (RMP1-14) only (n=3), CAR T cell only (n=3), and combination of CAR T cell and RMP1-14.
5. After randomization, treat mice with respective treatments:
    a. For CAR T cells: count and calculate so that the concentration is at 4e6 cells/200 uL for each mouse.
    b. For RMP1-14: inject 200µg/200µL to each mouse.
6. Three days post CAR T treatment, inject 200µg/200µL RMP1-14 to the respective treatment groups.
7. Six days post CAR T treatment, inject 200µg/200µL RMP1-14 to the respective treatment groups.
8. Image and measure tumors accordingly.
    a. Measure tumor growth with calipers twice a week.
    b. Image mice with Dluciferin and IVIS imaging system once a week.

Appendix II: Plasmids

1. 4H11-28z CAR construct in a SFG vector

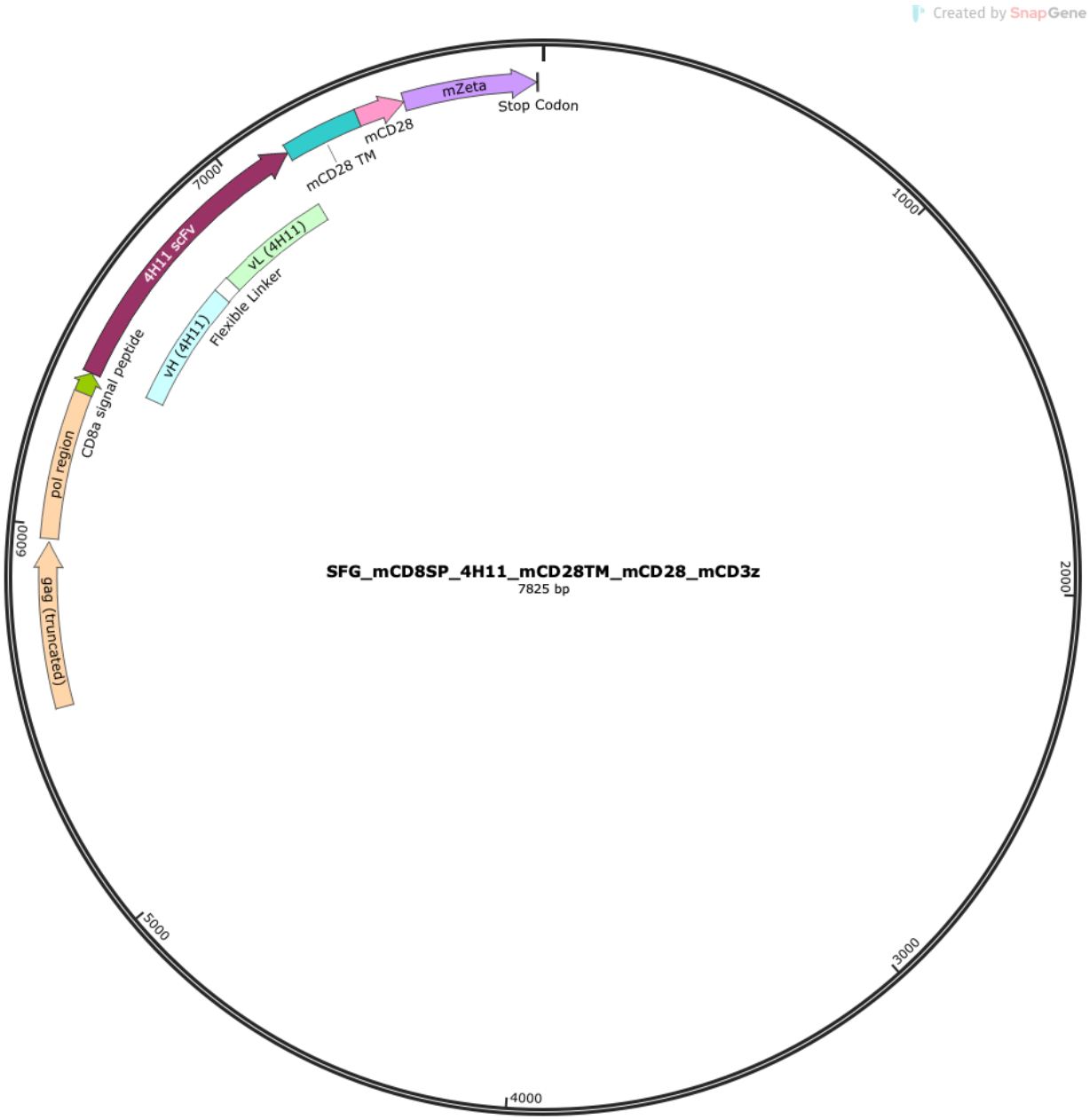

2. Close up of the SFG vector, 4H11-28z CAR

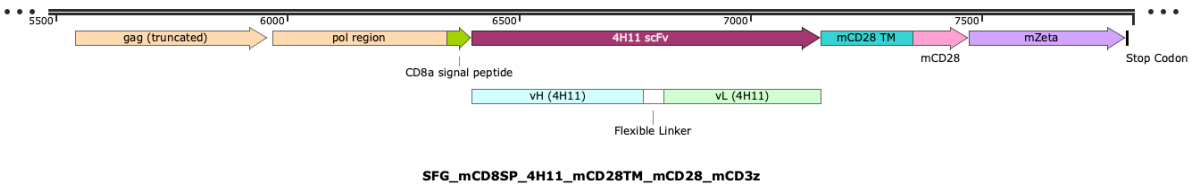

Appendix III: Supplementary Figures

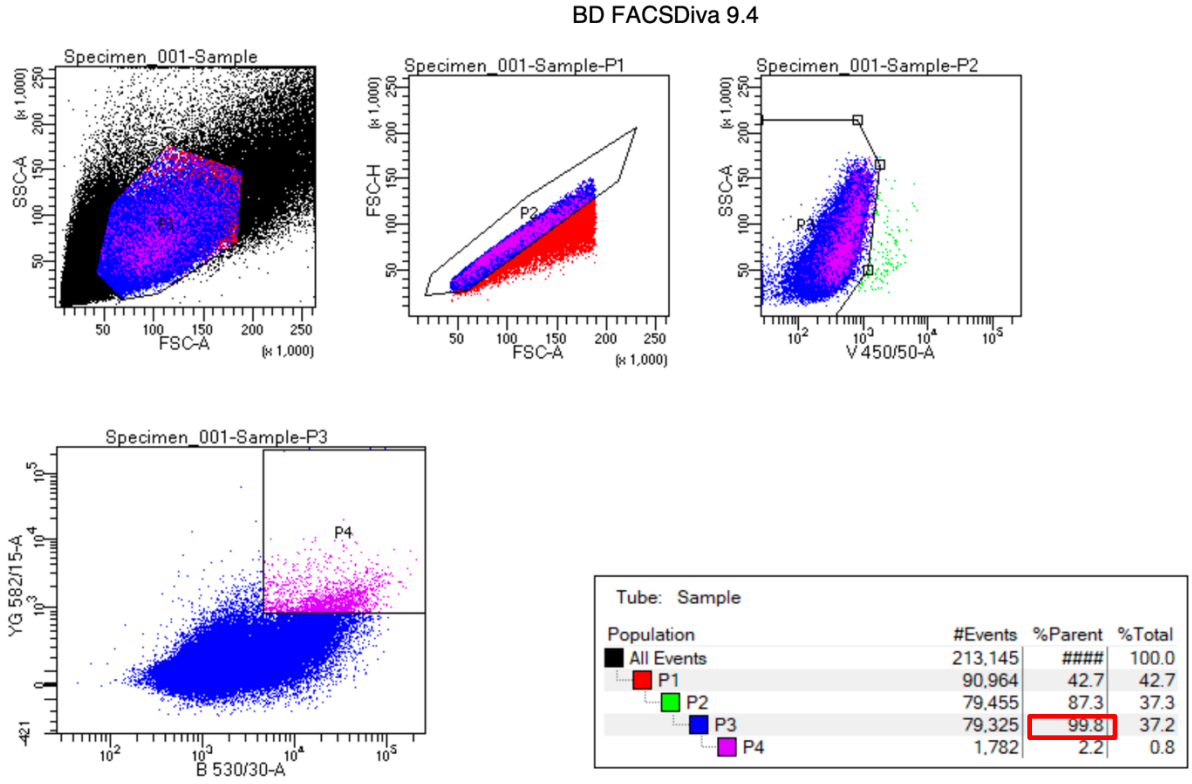

Supplementary Fig. 1: Facs sorted flow data depicting how Muc16CD-positive YUMM cells were sorted from the Muc16CD-negative YUMM cells before the *in vivo* study. YUMM cells were sorted with 99% Muc16CD+ cells and around 7×10^5 cells were able to be recovered.